000

735001

THE GEOLOGY AND GEOCHEMISTRY OF THE ZONED, Sn-W-F-Be SKARNS AT MT. LINDSAY, TASMANIA, AUSTRALIA

Teunis A.P. Kwak,
Department of Geology,
La Trobe University,
Bundoora, Victoria, 3083,
Australia.

ABSTRACT

The Mt. Lindsay Sn-W-F(-Be) skarns consist of discrete assemblages which show a distinct zonal pattern relative to the granite pluton's contact. From the edge of the skarn inward (approximately 200 meters from the pluton's contact) the zonal assemblages are: (1) F-vesuvianite + Ti-Sn-garnet ± Fe-pyroxene ± Sn-sphene ± scheelite (stage IB), (2) cassiterite + magnetite + ilmenite + siderite + quartz + K-feldspar ± danalite ± scheelite ± rutile ± ankerite (stage IA), (3) amphibole ± Sn-sphene + pyrrhotite ± magnetite ± ilmenite (stage IIA), (4) is like (3) except that Sn-ilvaite occurs (stage IIB), (5) is like (4) except that pyrite and arsenopyrite occur as matrix minerals (stage IIC), (6) annite + fluorite + quartz + pyrite + ilmenite (stage IID). Stage IB skarn forms a partial "mantle" around stage IA skarn. (1) and (2) (stage I assemblages) formed first with (3), (4), (5) and (6) (stage II) assemblages) progressively overprinting them. Assemblages (1) to (5) are all overprinted to varying degrees by annite, chlorite and stilpnomelane.

During stage II alteration, Sn-bearing silicates such as sphene (to 9.26 weight percent Sn), amphibole (to 0.79) and ilvaite (to 1.08) are produced by the reaction of stage IA assemblage causing all cassiterite to react and some Sn being lost to solution (average total Sn value of stage IA skarn ≃ 0.8; average of stage IID skarn ≃0.0).

Stage IA skarn genesis involved very low f_{O_2} values ($\lesssim 10^{-27}$), while that in the surrounding country rock is near $10^{-22.5}$ or higher at approximately 450°C. This suggests these primary, reduced skarn-forming solutions contained little meteroic water (which should be buffered at f_{O_2} values of the country rocks) and were largely derived from the ("A-type" granite) reduced, granite pluton. Stage II alteration occurred at relatively high temperatures (370-400°C) and only slightly higher f_{O_2} values.

INTRODUCTION

The characteristics of W-Sn-F replacement deposits are poorly known, particularly in the Western literature, because of their restricted geographical occurrences, complex structure, highly variable mineralogy and often sub-economic character. In Australia, examples of such deposits having minable ore include the tungsten mines of Kara, Tasmania (Wolff, 1978) and Molyhill, N.T. (Barracough, 1979), while tin mines include the very large Renison (Patterson et al., 1981), Cleveland (Collins, 1981) and Mt. Bischoff (Groves et al., 1972) examples in Tasmania.

In all of these, both sulphide-rich and magnetite-rich zones occur; the magnetite-rich zones commonly occurring nearest the pluton. In Australia, much effort by exploration companies has been exerted in finding cassiterite-sulphide replacement bodies "distal" from granitic contacts, the view being taken that sub-economic magnetite skarn-hosted tin and tungsten ore bodies occur closer ("proximal") to the pluton. It should be pointed out that this model has not been adequately tested and can not be substantiated by published data. In the Mt. Lindsay example, cassiterite-rich, magnetite skarn occurs farthest from the contact while sulphide-rich skarn occurs nearest the contact. The reason for this unexpected zonal pattern is the object of this study. The Mt. Lindsay skarns present an unique opportunity to study an example of such a W-Sn-F deposit because of their relatively simple structure and the large amount of drill core available affording an essentially three dimensional view of their occurrence and their relation to the accompanying pluton.

The term "Skarn" is here used in a broad sense meaning essentially "replacement of carbonate" or a replacement of a previous replacement of carbonate, whether Ca- or Mg- silicates are extensive or not (see Kwak and Askins, 1981b for discussion).

Location and Outline of Geology

The skarns occur approximately 15 kilometres north west of the large tin producing Renison deposit in the Northwest of Tasmania (G.R. 610 820, Burnie 1:250,000 sheet SK 55-3,also see Figure 1). The skarns occur in a sequence of steeply dipping sedimentary rocks with minor volcanics trending south-southeast (≈110°) approximately normal to the contact of a unit of the Meredith batholith.

The sedimentary rocks in the area consist of a monotonous sequence of greywackes, shales, minor volcanics and marbles. The sequence has a thickness of approximately 920 metres, consisting of seven formations or rock units (Jessop, 1969). At least part of the sequence is a stratigraphic equivalent to the Crimson Creek sequence found above the Renison Sn-sulphide deposit. The units at Mt. Lindsay are: the Parsons Hood beds (66 metres thick) - grey greywacke and shale; the O'Brien's formation (7-40 metres) - calcareous or dolomitic horizon; the Tullock formation (200 metres) - greywacke and grey shale; Mt. Lindsay formation (166 metres) - coarse grained quartzites and greywackes; Alston Volcanics (50 metres) - fine grained intermediate to basic volcanic flows and, possibley, some intrusive; the Neagle beds (166 metres) - greywackes, dolomitic shales, tuffs and red-brown shales; and, lastly, the Salmon Creek Beds (235 metres) - brown shale and greywackes. The skarns which were formed by the replacement of the O'Brien formation, extend out to a maximum distance of approximately 200 metres from the "Meredith granite" contact. They are believed to occur within the steeply dipping northeast limbs of a large anticlinal structure. However, axial plane cleavage has only been observed in a few shaley rocks. Postulated repetition of the upper part of the sequence in the immediate Mt. Lindsay area has been attributed to axial plane faulting of the anticlinal limb.

The associated pluton is inferred to be part of the Meredith granitic batholith which covers approximately 480 square kilometres and is ovoid in shape. The skarns occur on its southern margin while the important Cleveland deposit (see Collins, 1981) occurs near its northern margin. The batholithic rock near the skarns is biotite-poor granite which becomes both finer grained and porphyritic (K-feldspar and quartz) near the contact.

The medium grained rock consists of quartz, feldspar, biotite and rare rutile. The plagioclase (An_{10} to An_{25}), microcline-perthite and quartz form an even-grained mosaic. Biotite is late in the paragenesis with and rarely enclosed in quartz. When occurring as inclusions in late quartz it has a $^{Fe}/Fe + Mg$ (molar) ratio of near 0.88 (Table 1), relatively high F (to 2.11 weight percent), Cl (to 0.60 weight percent) and high Ti (to 2.84 weight percent). Significantly, biotites found outside quartz have low totals (approximately 90.00), and paler colours probably showing limited hydrothermal alteration to vermiculite? Such biotites are often associated with large rutile crystals. Within 20 metres of the contact biotite is absent. White mica alteration occurs throughout the granite sampled and is particularly concentrated within 30 metres of the contact, however, no true greisen occurs. The white mica has high FeO (to 3.96 weight percent), and SiO_2 (49.12), suggesting it is phengitic. The rock is here called a sub-greisen. Near the upper part of the granite, veinlets to 2 centimetres wide of quartz + dark, zoned tourmaline + fluorite + pyrrhotite ± chalcopyrite occur. Narrow syenite and granodiorite dykes have been described (Jessop, 1969) but were not observed by the author.

The bulk chemistries of seven granitic samples collected progressively up a granite intersection in ML35 indicate high SiO_2 (near 75 weight percent), high total alkalies and very low CaO, Fe_{total}, and MgO (Table 2). There is a relative enrichment of SiO_2 and a decrease of Al_2O_3 and Na_2O going up towards the contact. The bulk composition of the most unaltered rock is

essentially that of a granite (*senso stricto*).

The Skarn Deposits

The deposits consist of three explored parallel units and at least one unexplored one. The explored units from southwest to northeast are the No. 1 anomaly, Main Ore and No. 2 anomaly zones (Figure 2). Although adequate outcrops of the granite occur, the skarn outcrops are generally poor and highly weathered. Sufficiently definitive information could only be found from drill core data. Of these, the No. 2 anomaly was chosen for detailed work because here the drill core available was sufficiently evenly distributed over the length of the skarn and a large number (21) were available. The No. 1 anomaly and Main Ore zone units were not extensively studied because in the latter, although many drill holes are available (29), none occur near enough to the skarn-marble contact while in the former, there were not enough drill holes to indicate the extent of the skarn.

In the No. 2 anomaly unit, of the twenty-one available drill holes, eight evenly spaced drill holes occurring at increasingly greater distances from the skarn-pluton contact were chosen for detailed analyses (2/1, 2/5, 37, 47, 41, 38, 46 and 40, Figure 2). No drill hole closer to the pluton than 2/1 was chosen because the pluton contact dips shallowly to the south-east, the contact being just below the collar of this hole. In drilling, many of the drill holes were oriented so that the main ore zone unit, and lastly the No. 2 anomaly unit, were intersected in each hole with the result that many of the drill intersections in the No. 2 anomaly are relatively deep, near the end of the hole.

The fine grain size of the skarn hampered definitive macroscopic examination so that large numbers of polished thin sections were necessary. For each drill hole, core samples were routinely taken every meter of skarn intersection, although where observable variations occur, more closely spaced

intervals were chosen. Approximately 200 polished thin sections were made and all the opaque and non opaque minerals were identified by optical and election microprobe means.

Distribution and Mineralogy of Skarn Types

The fine grained nature of the skarns render definitive description of the core samples difficult. However, a rough macroscopic zonation can be defined. Nearest the pluton, nearly halfway down drill hole 2/1 to the bottom and at the very bottom of 2/5, a brown resinous, nearly pure biotite "skarn" occurs, having identifiable fluorite. A few greenish amphibole-rich areas partly altered by brown mica do occur in this skarn. Green amphibole + sulphide ± magnetite skarn occurs outward from the biotite skarn in the top half of 2/5, all of 37, 47 and the lower half of 41. Near the top of the 41 drill hole and in nearly all of 38, a grey coloured skarn occurs having a "salt and pepper"-type texture. Near the skarn-metasediment contact in drill holes 2/5, 47, 41, at the top of 38 and in 46, reddish garnet + dun-coloured vesuvianite-bearing skarn occurs. In drill hole 40, vesuvianite-bearing skarn occurs without red-brown garnet.

The distribution of primary and secondary minerals present in the skarn samples identified by microscopic means are shown in Figures 3 and 4 respectively. As will be discussed, the progressive alteration of "primary" skarn types to "secondary" skarn types has commonly been interpretted in other skarn studies (e.g. Taylor, 1976). These "stages" are often referred to as skarn or primary skarn stage and either as various "retrograde overprints" with "hydrothermal" stage elsewhere. Here, the first, or primary, skarn assemblage will be referred to as "stage I" skarn, secondary types, often containing relects of primary skarn, as "stage II skarn, and late, hydrous and fluorine-rich mineral alteration which overprints stage I and II, is referred to as "stage III" skarn.

Stage IA Skarn - cassiterite - siderite - K-feldspar - magnetite - ilmenite - quartz assemblage

Stage IA skarn is limited to the siderite- and cassiterite-bearing areas which is the "salt and pepper" textured skarn observed microscopically (see plate IIIB and Figure 3). Stage IB skarn is the vesuvianite-red garnet skarn. The former skarn type represents the major exploration target and occurs mainly near the outer edge of the ore skarn body. As can be seen in Figure 3, in addition to siderite + cassiterite, the unit also contains euhedral crystals of magnetite, ilmenite, danalite, K-feldspar, quartz, usually fluorite, more rarely scheelite, interstitial ankerite and Fe-rich calcite.

In thin section, magnetite usually occurs in cubic or polygonal shaped, atoll-like textures, in which the centres consist of grains or aggregates of siderite, K-feldspar, quartz or, more rarely, cassiterite (Plate IA). No ilmenite exsolution lamellae were observed (Plate IE). This magnetite contains only up to 0.09 weight percent Sn, to 1.19 TiO_2; to 0.51 Al_2O_3; to 0.88 SiO_2, and only to 0.05 MnO. Ilmenite forms as dispersed tabular prisms, some to 0.5 centimeters long (Plate IE), and again, having no observable exsolution lamellae. As impurities, ilmenite contains up to only 0.11 weight percent Sn; to 3.78, SiO_2; to 1.00, Al_2O_3; and, rarely, to 4.45 MnO, most MnO values being near 0.50 weight percent. On the basis of the analyses, temperature - f_{O_2} values are calculated as will be discussed later. Rare euhedral crystals of rutile occur within the siderite matrix. The rutile has to 0.58 percent FeO, 0.21 percent WO_3 but only 0.02 percent Sn as minor elements (Table 3).

Quartz and K-feldspar (orthoclase?), usually occur as isolated, clear, perfect euhedral crystals (Plate IB), and as interlocking mozaics of euhedral crystals in the carbonate matrix. K-feldspar contains up to 0.14 weight percent Na_2O; no CaO to 0.89, FeO; and to 0.73 F. To check these

unusually high F analyses, adjoining quartz and siderite were analyzed. These contained no F, suggesting F is replacing oxygen in the feldspar structure. Cassiterite occurs mainly as euhedral, short prisms in the siderite matrix and within the magnetite "atolls" (Plate IB). They are approximately 1.0 millimeters long and characteristically having dark brown cores and light brown edges. Quantitatively, it is very erratically distributed within stage IA skarn. Cassiterite contains up to 0.38 weight percent FeO; to 0.22, WO_3; to 1.03, F; and to 1.34, SiO_2 (Table 3).

The scheelite distribution is also highly erratic. Most scheelite occurs as single euhedral crystals, containing very little Mo (<1.0 weight percent) and anomalous fluorine (to 1.39 weight percent) as minor elements (Table 3).

Carbonates volumetrically make up the dominant minerals in the assemblage in most cases. Siderite, ankerite and calcite compositions are shown graphically in Figure 5. Both siderite and ankerite contain minor amounts of Mg (up to 10 and 18 mole percent respectively) with minor Mn. Siderite occurs as the dominant matrix mineral, in magnetite "atolls" and rarely, as radiating clusters of fine accicular crystals near the top of the DDH41 skarn intersection (plate IIF). In all the skarn types, calcite is the last major mineral to form and does so in late "vug-like" areas interstitial to nearly all other minerals and replacing early formed silicates (Plate IIE). Compositionally and texturally, it is distinctly different to calcite occurring in unreplaced marble (Figure 5). The skarn calcites are relatively Fe-rich, Mg-poor, while the marble calcites are nearly pure $CaCO_3$. No dolomite was observed anywhere in the area studied.

Danalite occurs in a few samples in cassiterite-bearing skarn (in ML.37). It is distinctive, occurring as pink masses and wedge-shaped crystals in handspecimen and having both Si and S peaks on the electron microprobe EDAX display. The Fe:Mn:Zn ratios are near 42.2:4.1:1 showing

the proportions of danalite:helvite:ghenthelvite. Other impurities in this mineral are negligible in amount. Flourite occurs in most samples in this skarn type as irregular masses and small cubic crystals in the carbonate matrix. 75 percent of cassiterite-bearing skarn has some degree of overprint by stage II or III assemblages.

Stage IB Skarn - vesuvianite - garnet - calcite assemblage

This skarn type occurs between the stage IA skarn and: (a) enclosing pelitic country rocks in many areas, and (b) unreplaced marble. Its distribution is best shown by the distribution of Fe-vesuvianite (Figure 3) which shows it to be, partially, a mantle around the Stage IA and relict IA skarn types. It is distinct from vesuvianite-grossular garnet "metamorphic" skarns present in unreplaced marble. Vesuvianite derived solely by contact metamorphism occurring in DDH 40 is different by having much lower F (Table 4).

The stable assemblage in vesuvianite skarn is vesuvianite ± red ± garnet ± sphene ± scheelite ± calcite ± pyroxene. Noteably, no cassiterite, K-feldspar, quartz or siderite were observed in this skarn type, just as no vesuvianite, pyroxene or garnet occurs in the cassiterite-siderite skarn.

Vesuvianite occurs as interlocking large, growth zoned prismatic crystals or as radiating clusters consisting of tabular to accicular crystals (Plate IIA). Compositionally, vesuvianite is relatively homogeneous in composition (Table 4), having Fe/Fe + Mg near 0.55 (molar), F values to 1.62 weight percent and Ti of up to 4.27 weight percent. Little variation exists between core and rim compositions (Table 4).

Red-brown, colour zoned, garnet occurs sporadically in Stage IB skarn. The Fe-rich garnet is unusual in often being very high in Ti (to 5.42 weight percent). Sn (to 0.51 weight percent, see Figure 7), and

F (to 0.36 weight percent). Noteably, the highest Ti values occur in garnets located at the outer edge of the skarn away from the granite contact (DDH46). Significant compositional variations occur in different colour (and growth zones) in the garnet, garnet midsections often being most Ti-rich (Table 4). Pyroxene is only present in a few samples. It is characteristically hedenbergite-rich (Table 4).

Both scheelite and sphene are erratically distributed in vesuvianite skarn. Scheelite is normally very low in Mo (< 1.0 weight percent) and characteristically is high in Sn, Al_2O_3, and FeO (see Table 3). Fluorite is generally absent from this skarn type. Late calcite filling vug-like areas occur between the silicate minerals.

Vesuvianite (-garnet) skarn in some places has been overprinted by some minerals characteristic of stage IA or IIA mineralogy. In these cases, vesuvianite and garnet crystals are found embedded in a magnetite matrix (Plate IIC). This phenomena was only observed in vesuvianite (-garnet) skarn samples nearest the pluton (in DDH 37 and 2/5). Vesuvianite skarn is also extensively overprinted by stage II alteration (see Plate IIC and Plate IIB). The massive magnetite overprint in Plate IIC may, actually, relate to stage II skarn as will be discussed later. Stage IB skarn does not overprint stage IA skarn.

Stage IIA Skarn - Amphibole- Pyrrhotite - Sphene assemblage

This green amphibole skarn type occurs closer to the pluton adjacent to stage IA skarn. Its distribution is best defined as the area where green amphibole exists without the presence of ilvaite or pyrite as a matrix mineral (Figure 4).

Amphibole occurs as an alteration of the silicates in both stage IA and IB skarns, although in the former, no pseudomorph after such minerals as K-feldspar and quartz were observed. In this case, amphibole probably nucleated in the siderite matrix adjacent to magnetite. In Stage IB skarn,

amphibole commonly forms as a pseudomorph after both vesuvianite (Plate IIB) and garnet (Plate IIC).

Both green to blue-green and very pale green to colourless amphiboles occur in stage II skarn. The latter usually forms as a thin rim around crystals of the former and more rarely as crystals postdating the darker green variety (Plate IIE). The distribution of the two amphibole types is shown in Figure 4, while compositions, in Figure 6. The dark green variety is ferrohastingsite with average F:Cl:OH proportions of near 0.76:0.14:0.09 and Sn values up to 0.79 weight percent but usually near 0.3 weight percent (Table 5). The pale variety is essentially (actinolite-) tremolite in composition with very low Sn values, up to 0.10 weight percent. Pyrrhotite occurs everywhere in the stage II skarns except in the annite-fluorite skarn (stage IID). It appears cogenetic with amphibole and has Cu = 0.17, Mn = 0.02, and extremely low Sn (0.02 weight percent). Chalcopyrite is similarly distributed to pyrrhotite (Figure 4), except that it does not occur in unreplaced marble. Compositionally it has Mn = 0.04 and no Sn, even when found adjacent to stannite (in fractures in stage IA skarn).

Sphene occurs throughout stage IIA, IIB, IIC and IB skarn (Figure 5). It formed mainly after ilmenite (Plate IE) in amphibole-bearing skarn and as large single crystals in IB skarn. The composition of sphene varies greatly, Sn values occur as high as 9.26 weight percent with average values near 1.00 to 2.00 (see Figure 7); Fe ranges to 3.48 weight percent, and, Al to 7.49 (Table 5). Both fluorite and quartz occur as interstitial masses to amphibole while calcite, texturally, is the last mineral to crystallize.

Stage IA and IB minerals occur as corroded relicts in some stage II skarns. Corroded K-feldspar, siderite, cassiterite (Plate 1C, 1D) and quartz crystals occur only near the stage I - stage II interface in DDH 41.

Siderite and K-feldspar occurs very rarely, followed by cassiterite while partly altered euhedral quartz is more common. Relict magnetite and, to a lesser extent, ilmenite, are common in stage II skarn. Fairly large areas of danalite occur in some relict stage IA skarn. Bulk analyses of meter long sections (DDH 37) have maximum Be values of 300 ppm. In many stage II skarn assemblages, magnetite occurs as large homogeneous masses rather than the smaller, often atoll zoned grains observed in stage IA skarn. As such, magnetite in stage IIA skarn may be, in part, produced during this stage while in stage IIB it clearly appears to be reacting, in part, to ilvaite as will be shown.

Both garnet and vesuvianite relicts are common in stage II skarn, their replaced relicts are also very obvious. (plate IIC, IID)

Stage IIB - Ilvaite - Amphibole - Pyrrhotite assemblage

Stage IIB skarn is similar to stage IIA skarn, except that the mineral ilvaite occurs ubiguitiously and no interstitial pyrite occurs (Figure 4B). Ilvaite's identification was confirmed by X-ray diffraction. It characteristically occurs as fine, dark brown elongate crystals and fibers, commonly in fluorite, as well as aggregates of elongate bladed crystals mantling and altering relict magnetite (Plate IID).

When it occurs as long, thin brown fibers, it very much resembles fibrous cassiterite and could easily be mistaken for such. Compositionally the mineral contains more Sn than amphibole (to 1.08 weight percent - see Figure 7); Al_2O_3, to 7.30; low F ≈ 0.30 and nearly no Cl (Table 5). Because both Fe^{+3} as well as Fe^{+2} occur which could not be analyzed by the method used, OH values and totals are probably not very reliable. Ilvaite does not occur in stage II skarns which can be shown by textural data to have formed from stage IB skarns, possibly due to the absence of available relict magnetite.

Stage IIC - Pyrite - Ilvaite - Amphibole - Pyrrhotite (-Arsenopyrite) assemblage

This skarn occurs nearer the granite than stage IIB skarn and mineralogically is similar to stage IIB skarn except that pyrite and, usually, arsenopyrite occurs (Figure 4). Pyrite occurs as a matrix mineral not only in veins as it does in most of the other skarn types (Figure 4). Pyrite is relatively pure, having up to 0.37 weight percent Zn; to 0.60, Cu; to 0.14 Mn; and less than 0.02, Sn. Arsenopyrite contains up to 0.14 weight percent Zn; to 0.15 Cu; to 0.02, Mn; and up to 0.08 Sn. Relict stage I skarn textures are rare in stage IIC skarn.

Stage IID - Annite - Fluorite "Skarn"

This skarn type occurs mainly in a zone nearest the pluton (Figure 4). In handspecimen, it has a distinctive brown resinous appearance; annite exceeds 75 modal percent. The evidence that stage IID is produced from previous stage II skarn types is not obvious in many samples, however, green amphibole-rich areas partly altered to annite occur in parts of stage IID skarn (in DDH 2/1). Annite overprints nearly all skarn types (see Figure 4) and the pattern of progressive alteration going into the granite is similar to that observed in small scale samples (Plate IIIB).

Annite occurs altering any previous Fe-bearing mineral including magnetite, ilmenite, Fe-silicate or possibly, siderite. However, only in the stage IID skarn area (shown in Figure 4) has replacement been complete. Texturally, it commonly occurs in fractures between silicate minerals. Annite contains up to 36.22 weight percent FeO; to 8.18, MgO; to 0.43, MnO; and to 2.05 TiO_2 (Table 1). The highest Sn value was 0.12 weight percent but nearly all values were in the range 0.00 to 0.03.

The mineral is usually sector zoned (see Kwak, 1982). In each sector, the highest Mg + Ti values occur near the dark brown centres of crystals with Mg + T values, colour intensity and the degree of brown colour decreasing

outward. Mg + Ti values in the (001) sectors are much lower than in the (010) and (100) sectors. Structural formulae calculations are satisfied by filling the tetrahedral positions with Si, Ti and Al. A small amount of Al also enters the octahedral position with Fe^{+2}, Mn, Mg and Zn.

Stage III skarn - late hydrous- and fluorine-bearing minerals

These minerals of various types probably represent a sequence of alteration in themselves. The distribution of stilpnomelane and chlorite in Figure 4 reflects permeability and the availability of materials reactive enough late in the deposit's genesis, that is, mainly unreplaced state IA skarn. In the stage IA skarn, this alteration occurs mainly in the siderite matrix or rarely, mantling siderite rosettes (in DDH 41- Plate IIF). The alteration also occurs rarely in "vuggy" areas between amphibole in stage II skarn. The compositions of typical chlorite and stilpnomelane are listed in Table 1. Apophyllite (Table 5) has been identified in a number of samples as a late vein filling.

Orientation of the Skarn Zones

The data in the last section was collected from inclined drill holes many of which intersected first the Main Ore zone and later the No. 2 anomaly, drilling from southwest to north east, at orientations which were approximately in a plane normal to the strike of the units. In the mineral distribution patterns in Figures 3 and 4, the "out" isograd (out from the pluton) of a mineral such as ilvaite, intersects the plan projection (along the strike of the beds) at shallow (acute) angles (angle α in Figure 8). Geometrically, this must mean that the plane of the "out" isograd of the mineral must approximately be parallel to the granite's contact, the contact dipping gradually to the east (Figure 8). Nearly all the mineral distribution patterns in Figure 3 and 4 show this trend which must indicate that in a section taken along the strike of the units, successive alteration of the primary stage I skarns occurs progressively

going in towards the pluton (figure 8). This is diagrammatically shown in Figure 11 in a longitudinal section.

There are clearly some noteable exceptions to this. The distribution of cassiterite shows (a) an area near the bottom of DDH 37, off the Figure 9 longitudinal section, and (b) also, not discussed here, near the contact with the granite (in DDH 35 - Main Ore zone). Like the green amphibole within stage IID skarn, these occurrences must be viewed as being reaction remnants, in every case they are partly or largely altered to a later skarn assemblage. Such remnants probably occur elsewhere in the skarns, the original alluvial mining of cassiterite at the "Mt. Lindsay" mine probably represents a weathered one of these. These remnants occur because enough required permeability did not develop in that part of the skarn during stage II or stage III alteration for complete reaction to have occurred.

Compositions of the Skarn

Bulk analysis of the skarns were not attempted in this study, but analyses were done by Kinealy (1979) from the same drill holes used in this study with their exact location given. In Kinealy's study, the zonation present in the skarn had not been identified, although approximate mineralogical descriptions are given. Many of the samples used in the present study come from within a metre of those analyzed by Kinealy. The results of Kinealy's study, listed in Table 7, should be viewed only as partial analyses as will be explained.

The totals for the amphibole-bearing skarns 64260, 64261 and 64267 and the annite "skarns" 64262 and 64263 are too low to be normally acceptable. Kinealy infers that deviations of greater than 2 percent from 100 are due to high iron values, the error probably being due to the determination of that element. He does not confirm this inference by additional analysis, however. The samples which have low totals all have very high modal proportions of Cl- and S-bearing minerals. Also, as shown in Figure 4, arsenopyrite (As) and chalcopyrite (Cu) are

concentrated in some amphibole-bearing skarn. In most cases, the annite "skarn" consists of over approximately 75 volume percent mica which commonly contains over 1.00 weight percent Cl + F (Table 2). Thus, if Cl had been analysed by Kinealy, the totals would have been considerably higher (near 99 weight percent totals for most). Amphibole routinely contains approximately 1.00 weight percent Cl and usually totals at least 50 volume percent of the amphibole-bearing skarns. Thus, those samples should be at least 0.5 weight percent higher. Combined Zn, W, Be, As and Cu in most rocks would probably account for another 0.2 to 0.5 weight percent (the Zn content of amphibole is up to 0.12, W is up to 0.17).

In the bulk chemical analyses of complex rocks such as these which contain high F etc., it is incorrect to assume all Ca, for example, occurs as CaO. In fact, some will occur as CaF and some Fe will be as FeS_2, etc. Bearing this in mind, and assuming that (a) the small core samples used are truly representative of the skarn types, and (b) any original chemical differences between the (pre-skarn) carbonate rocks were minor, the following generalizations are made.

Relative to stage IA skarn, stage IB skarn is enriched in SiO_2 and CaO with TiO_2, CO_2 and MgO also being high in some examples, while K_2O and FeO + Fe_2O_3 are lower. High Sn in stage IB skarn is related to high modal abundance of garnet (and high Fe^{+3}/Fe^{+2} values). High Sn, F, and Fe proves this skarn is a product of the ore skarn genesis. Going from stage IA to stage IIA, there is mainly an increase in Fe_2O_3 + FeO with decrease in Sn and W, generally. The two stage IIA samples may be biased in having had very high original (relict?) magnetite contents or, as inferred previously, massive magnetite actually crystallizes during stage II genesis.

Going from stage IA to IIC, there is a decrease of K, CO_2, and, in part, Sn, with an increase of CaO, Fe^{+2}/Fe^{+3}, SO_3, Na_2) and MgO. These trends are also supported by mineralogical and textural differences

cited; stage IA skarn is rich in magnetite (Fe^{+2}/Fe^{+3} = 2), K-feldspar (K), siderite (CO_2) and cassiterite (Sn), while stages IIA to IIC are rich in amphibole (Mg, Na, Fe^{+2}) and sulphides (S). The stage IID skarn consists mainly of annite, although some annite alteration does overprint some of all the earlier skarn stages. Relative to earlier stages, the stage IID skarn is enriched in F, $H_2O_{(total)}$ and K_2O with decreased Na_2O and Sn. This trend with respect to Sn, W, Cu and Zn is also shown in Figure 9.

During assessment of the drill core many elements of economic interest were analyzed, tin was determined as total Sn (by X-ray fluorescence) and acid soluble Sn (by acid leaching). The assumption is usually made that acid soluble tin reflects the stannite content, cassiterite being essentially insoluble. In Figure 9, it can be seen that Sn_{total} values are highest in stage IA skarn (most of DDH 39, part of DDH 41), low in the stage IB (DDH 46) and variable but relatively low in the drill holes having mainly stage II skarns. Sulphide contents are highest in the stage II skarns (see Figure 4), but the only place stannite was observed was with chalcopyrite in fractures in stage IA skarn (Figure 4). Noteably, where high $Sn_{soluble}$ occurs, there is no observed stannite, but large amounts of Sn-sphene and Sn-ilvaite occur. It is suggested that Sn-sphene is the main source of $Sn_{soluble}$ in the Mt. Lindsay skarns.

Tungsten values are erratic, highest values occuring in DDH 37, partly altered stage IA skarn, and in DDH 38 (mainly stage IA skarn). Copper has highest values in DDH 38, where some very high grade sections of chalcopyrite + stannite fracture fillings occur. These fractures cut stage IA skarn, unaltered stage IA skarn generally contains no sulphides. Arsenic distribution is fairly evenly distributed, the high values are mainly due to fracture filling arsenopyrite. As can be seen, bismuth is appreciable, to 0.044; Zn, to 0.24; Pb, only to 0.012; Ag, to 9 ppm and Mo, to 0.002.

Permeability

The mechanisms necessary to produce required permeability in garnet-pyroxene-scheelite (tactite) skarn elsewhere is at least partly by dissolution of $CaCO_2$ to produce Ca(-Fe) silicates + $CaCl_2$ + pores, and, probably, fracturing (Taylor, 1976; Kwak and Tan, 1981). The pore space produced is often observable by late "vugs" of calcite, quartz, or Fe-oxides. As has been clearly demonstrated in the case of the King Island skarn deposit (Kwak and Tan, 1981), permeability changed during skarn genesis. Previous open spaces being during Ca + Fe silicate precipitation and ultimately closed by late, low temperature, calcite or quartz precipitations. Thus, present-day permeability is not a good indication of permeability present during genesis.

Permeability in fluorine-rich, magnetite ("wrigglite") skarns is produced by a mechanism of periodic fracturing with replacement proceeding up to approximately 5 centimetres out from each fracture by a Leisegang-type diffusional mechansim (Kwak and Askins, 1981a, b). In granular magnetite-fluorite skarns, or amphibole-rich skarns, no mechanism has been suggested.

In the present study, some vug-like areas of late calcite occur in both stage I and stage II skarns, suggesting open space existed. However, the spacing of fractures in both skarn types, but particularly the former, is particularly prevalent. In stage IA skarn, there are 98.4 fractures per metre of core length (average of 25 metres), while in unreplaced marble, this is only 25.7. There is no apparent increase of fracturing with proximity to the pluton's contact. The mechanism suggested is that some dissolution of $CaCO_3$ with periodic fracturing produced the required permeability. Presumably, P_{CO_2} builds up by replacement of carbonates to the point that the breaking strength of part of the skarn or skarn-to-be unit is exceeded. After failure of the rock and fluid pressure release a zone of "crackling" proceeds that of skarn replacement, the

shape of each increment of newly produced carbonate rock suitable for skarn replacement, depending partly on the rock's breaking strengths. Such periodic fracturing is well shown in related "wrigglite" skarn (see Kwak and Askins, 1981a, b). Permability necessary for later skarn replacement is in some cases by reopening previous fractures partly sealed by previous skarn minerals. Thus, in Plate IIIB, annite has replaced green amphibole along a fracture through pelitic rock. Amphibole has partly replaced a thin magnetite skarn layer, the amphibole forming interstitial to large magnetite masses. Annite in the layer is interstitial to the amphibole.

Conditions of Formation

In many hydrothermal systems, fluid inclusions are considered to be the most diffinitive in determining temperature-fluid composition conditions (i.e. Kelley and Turneaure, 1970; Kwak and Tan, 1981), but suitable fluid inclusions are absent in the Mt. Lindsay skarns. Very minute, saline (60 weight percent total dissolved salts?) inclusions occur in rare danalite. The lack of suitable fluid inclusions here in contrast to other skarn environments (i.e. see Kwak and Tan, 1981), may be due to the lack of a dynamic enough process during genesis, such as is probably produced during the boiling of hydrothermal solutions.

The author is very skeptical of using solid phases to determine approximate P-T conditions, because of (a) large uncertainities in most experimental work, (b) impurities in natural minerals not accountable for when using experimental results, and (c) textural problems in identifying truly stable assemblages.

In spite of this, the following approximations are tentatively made. Coexisting ilmenite + magnetite are common. Ilmenite-hematite and magnetite-ulvospinel solid solution contents are unfortunately too low to plot on Lindsley's 1963 diagram. If the curves on his diagram

are extrapolated as in Figure 10A, values in the vicinity of 400° to 450°C and log f_{O_2} values of 10^{-25} to $10^{-27.5}$ are inferred for stage IA skarn (in DDH 38, 41 and part of 47). In DDH 37, 2/5 and 2/1 ilmenite-magnetite relicts were analysed and these values probably refer to stage IA skarn in these areas prior to stage II alteration.

The occurrence of siderite + magnetite and no hematite or graphite, can be used with French's 1971 data to infer a log f_{O_2} of approximately 10^{-25} to $10^{-26.5}$ and temperatures of 360° to 450°C at 500 bars (CO_2) pressure for stage IA (Figure 10B). The equilibria is not very much affected by higher pressures (to 2000 bars). The results are consistent with the ilmenite-magnetite data, the values probably being near the upper temperatures and lower f_{O_2} values. In terms of log f_{S_2} - log f at 400°C, the stage IA skarn probably plots at log f_{S_2} values near or below 10^{-10} to 10^{-15} (Figure 10C).

The conditions for stage IB skarn is less defineable because of the deviation of the garnet from ideal andradite. Nearly pure hedenbergite + quartz + magnetite + andradite (solid solution) garnet co-exist rarely, usually magnetite + quartz are absent in the assemblage and vesuvianite is present instead of hedenbergite. Assuming Sn and Ti behave similar to Fe^{+3} in the andradite structure, and using 400°C as the temperature of formation (derived from information from stage IA skarn data), a log f_{O_2} of $10^{-27.5}$ is derived for the few samples which have the assemblage (Figure 10D). The occurrence of some Sn solid solution in sphene (commonly near 3 weight percent) with no malayaite and Takenouchi's 1971 data limits the temperature as being above approximately 300°C, for stage IB (and stage IIA, IIB and IIC skarns generally).

The occurrence of pyrrhotite + magnetite in stage IIA skarn is possibly not a stable assemblage, but assuming a close approach to equilibrium exists, log f_{S_2} values at 400°C would be less than approximately

10^{-9} (Figure 10C) with log f_{O_2} values between 10^{-27} and 10^{-30}. Pyrite + pyrrhotite + magnetite in stage IIC skarn is also probably not a stable assemblage, magnetite being consumed. If conditions were near the equilibrium curve (Figure 10C), and if the temperature was approximately 400°C, a log f_{O_2} of approximately 10^{-26} applies. In Figure 10C a log f_{S_2} value of $10^{-12.5}$ applies.

The assemblage, nearly pure K-feldspar + magnetite + biotite is common in partly altered stage IA skarn but no hematite occurs. K-feldspar + magnetite are clearly relict to biotite here. Using Wones and Eugster's 1965 data (at P_{H_2O} = 2070 bars), for Fe/Fe + Mg values of 0.9, log f_{O_2} values of from $10^{-19.5}$ to $10^{-17.5}$ at temperatures of from 370° and 725°C are inferred. The lower value is most probable. The data may not apply if high salinities are present and calculating f_{H_2O} values under such conditions using their data is suspect or if a close approach to equilibrium has not been met.

Pyrite, but no pyrrhotite, occurs in stage III skarn, suggesting log f_{S_2} values greater than $10^{-12.5}$. The assemblage hematite + magnetite occurs in some of the subgreywackes marginal to the skarns. With the hematite-magnetite curve (Figure 10C) at 400°C, a value of 10^{-22} applies.

DISCUSSION

The evolution of the skarns at Mt. Lindsay involved significantly changing conditions. Early stage IA and IB skarns are closely related. Stage IB is not simply metamorphic in origin because it contains anomalous Sn, W, and Ti (Table 7). $Fe^{+3}/Fe^{+2} + Fe^{+3}$ values in stage IA are much higher than in stage IB skarn, implying possible higher f_{O_2} values there. The mantling of stage IA skarn by IB skarn may represent a zone of mixing between relatively high f_{O_2}, low Fe + Ti constituents fluids derived from the country rocks and low f_{O_2}, high Fe + Ti fluid related to the granite intrusion. However, implications from mineral chemistry (previous section) do not confirm this view; f_{O_2} values in stage IA and stage IB seem

very similar, although there are serious limitations on the f_{O_2} value determinations in stage IB skarn as discussed. Perhaps the IA and IB skarns are different due to $^{a}Fe^{+2}$, $^{a}Fe^{+3}$, $^{a}SiO_2$ or some other activity difference(s). No quartz was observed in stage IB skarn and the activity of silica there may have been lower than stage IA skarn where quartz occurs.

The stage II skarns formed progressively form the granite's contact out both in time and space (Figure 11). Amphibole skarn forming after an earlier skarn consisting of largely an anhydrous assemblage is common in skarn studies (i.e. the "stage II" skarns of Taylor, 1976). The relationship between the two has been interpretted in two ways. Nockleberg (1981) believes amphibole found nearest the pluton at the Strawberry mine (Calif., U.S.A.) is a progressive replacement of pyroxene skarn (Zone 3) which in turn is formed after garnet skarn (Zone 2). The relationship is similar to that proposed by Zharikov (1970) and Korzhinskii (1964, 1970). It is implied that the progressive replacement does not involve discontinuous changes in temperature or fluid composition. However, oxygen and deuterium isotope evidence on amphibole skarn by Taylor and O'Neill (1977) in the Osgood Mountain area (Nevada, U.S.A.) suggests meteroic water comprised 20 to 50 percent of the fluid during amphibole skarn (stage II) crystallization with temperatures near 480° to 550°C, while during pyroxene + garnet skarn (stage I) the fluid was primarily derived from the primary magma (δ^{18} = 7 ‰ δD_{calc} = -45) and temperatures in excess of 550°C occurred. Data on fluid inclusions by Kwak and Tan (1981) on the King Island Scheelite deposit agree with this conclusion. At King Island early garnet-pyroxene skarn (stage I) nearest the pluton formed from fluids at 600 to 800°C and salinities of approximately 14 to 16 molar (average) while amphibole (stage II) had temperatures of less than 500°C and salinities of approximately 6.54. Unlike Nockleberg's and Korzhinskii's inference, these data imply amphibole skarn is a late event during genesis with there being a distinct

fluid composition and to a lesser extent, a temperature break between stage I and stage II alteration. Similarly, the interpretation favoured at Mt. Lindsay is that stage II skarns overprinted stage I skarns after significant amounts of meteroic water had mixed with primary (stage I) skarn fluids. The source of this alteration was along and out from the pluton contact. Some stage II skarn assemblages overprint previously formed stage II assemblages, for example, annite (stage IID) overprints all the stage II skarn as well as unaltered stage IA skarns (but generally not unaltered stage IB skarn).

Mineralogical and chemical zonation of skarn deposits relative to the associated pluton are quite variable. In many, however, a secondary hydrous amphibole ± epidote skarn occurs nearest the contact and overprints a primary anhydrous skarn farther out (e.g. Strawberry Mine, Calif., U.S.A., Nockleberg, 1981). In a few, a biotite-rich zone is reported between the pluton and the amphibole zone. In the copper skarns at Carr Fork, Bingham, Utah, U.S.A. (Atkinson and Einaudi, 1978) dark brown (annite?) mica post dates actinolite alteration (p. 1345) which in turn alters actinolite-diopside-quartz skarn (p. 1346) generally out from the pluton. At Sandong, Korea (John, 1978) there is a very distinct inner biotite-rich zone followed by a hornblende-rich zone concentrically around it followed by a concentric outer (primary) garnet-diopside zone. This is explained by progressive hydrothermal alteration of the primary skarn (John, 1978, p.200). Biotite alteration after amphibole is also extensive at the nearby Cleveland Mine, Tasmania (P. Jackson, *pers. comm.*, 1982).

The evolution of Mt. Lindsay involved increasing f_{S_2}. Stage IA skarn has magnetite with no primary sulphides; IIA and IIB, pyrrhotite + (relict?) magnetite; IIC, pyrrhotite + pyrite + (relict?) magnetite; and IID, pyrite with no magnetite. Similarly, there is an increase of hydrous minerals. Unaltered stage IA skarn is anhydrous; IIA has amphibole; IIB and IIC, amphibole + ilvaite; and IID, annite.

This may be due, to a large part, to dilution or mixing of highly saline, pluton-derived (high Fe + Ti + Sn, low f_{O_2}) water with dilute meteoric water rather than a temperature decrease. The calculations in the last section suggest similar temperatures during stage I and most of stage II genesis. Also, ferrohastingsite having very similar compositions to those in the skarn and formed at magmatic temperatures are known in some alkali ("A"-type) granites (Collins et al., 1982). The activity of H_2O in a very saline solution (e.g. 65 weight percent, total dissolved salts) would be much lower (< 0.8) than in dilute solutions and crystallization of a hydrous phase would be inhibited.

The relatively high Sn and W concentrations in magnetite-bearing stage IA skarns relative to garnet-bearing stage IB skarn, has been observed in other Sn-W-F(-Be) type skarns (i.e. Barraclough, 1979; Wolff, 1978; Kwak and Askins, 1981b) and may suggest log f_{O_2} and/or pH (≃ acidity at high temperatures) values were already too high for significant amounts of these elements to remain in solution even before conditions to produce stage IB skarn occurred (see Eadington and Giblin, 1979 for Sn-solubility in f_{O_2}-pH space). Any Sn which remained in the solution which formed the stage IB skarn crystallized mainly in Ti-Fe(-Sn) garnet and, to a lesser extent, Sn-sphene rather than cassiterite here.

Scheelite and cassiterite precipitating during stage IA skarn genesis must have been redissolved and reprecipitated elsewhere. The evidence for this is (a) cassiterite arrested breakdown textures are common in DDH 41, at the stage IIA - IA interface, and (b) although relict stage IA minerals and textures exist in some stage II skarn, relict cassiterite is absent along with K-feldspar + siderite. The occurrence of high Sn or W values some distance out from the granitic contact and often near the skarn's edge, is a common feature in skarns (i.e. Umpleby, 1916; Temp Piute, Nev., U.S.A. - Buseck, 1967; King Island

Scheelite, Tas., Kwak and Tan, 1981; Kara, Tas., Kwak et al., 1982). The available data suggests stage IA, stage IB and most of stage II skarns formed under similar temperatures and not greatly different f_{O_2} values. To explain cassiterite precipitation and dissolution, genetic models based on changing pH (≃ acidity at high temperatures) and changing ionic strength are suggested. Figure 12A shows the relation of pH, log f_{O_2} and Sn_{Total} solubility for the sum of the activities of the $SnCl_2^\circ(aq)$ and $SnF^+(aq)$ complexes at activity of Cl^- = 1 and activity of F^+ controlled by fluorite (after Eadington and Giblin, 1979). $SnCl_2^\circ$ and SnF^+ are the main species in solution at low pH values. A low pH, Sn bearing solution at 400°C (point 1, figure 12A) encountering marble would be largely neutralized (point 2) and essentially all Sn would precipitate. Comparing diagrams 12A and 12B it is obvious that simply cooling the solution would precipitate tin but the geological evidence cited does not uphold this view. Whether this primary solution was saturated in Sn prior to reaching the carbonate is unknown but it could well not have been. As long as $CaCO_3$ was present, the system probably approximated a pH (≃ acidity at high temperatures) trap to passing Sn-bearing solutions. When all the marble-derived calcite had reacted, this buffer was no longer present. New increments of fluid, probably undersaturated in Sn (+ W) in the now unbuffered (calcite-free) skarn would not precipitate cassiterite + scheelite until new marble calcite is encountered, at the skarn-marble interface. Where suitable permeability existed in calcite depleted stage IA skarn, scheelite + cassiterite would be leached if the primary solutions was undersaturated and reprecipitated at the skarn-marble interface. Thus, a zone of high Sn + W would move outward during the skarn's genesis. Conversely, on dilution of a Sn-bearing solution at a temperature of 500°C, f_{O_2} of 10^{-27} and pH of 3.5 (figure 12C), tin would precipitate. For this to happen pH and f_{O_2} would have to be affected.

The model favoured is the first. The model would explain the

irregular distribution of Sn + W in stage IA skarn at Mt. Lindsay, areas of low Sn being relatively leached stage IA skarn (such as is represented by analysis 15, table 2). Whether the leaching event predated or was coincidental with stage II alteration is not known. During stage II alteration, various Sn-bearing silicates such as Sn-sphene, Sn-ilvaite and Sn-amphibole crystallized from stage IA and IB skarn. Whether cassiterite relicts (Plate IC, ID) actually represent remnants retained after the leaching event hypothesized but prior to stage II alteration is unknown.

The alteration of stage I skarns to stage IIA, IIB and IIC skarns probably involved the loss of some Sn (+ W?) while during stage IID alteration, essentially all Sn (+ W?) was lost. It is suggested that this Sn is lost to the fluid phase and reprecipitated in an areas now lost to erosion. Whether this would form an economic deposit itself or be disseminated would depend on local geological features. It is possible that the high Sn zones in the upper part of the Cleveland deposit (Luina, Tas., Collins, 1981) represent such a situation. Primary amphibole-magnetite-cassiterite-danalite-annite exist at depth at the Cleveland deposit while in the upper levels, up to 800 meters vertically above amphibole skarn, chlorite-pyrrhotite-cassiterite skarn occurs (P. Jackson, *pers. comm.*, 1982). At Cleveland, the latter rock type, which is the main Sn ore, appears to be mainly associated with relatively low angle faults. This implies low angle fault(s) at Mt. Lindsay may be prospective.

The Main Ore zone skarn contains no known large discrete stage IA skarn areas inspite of the fact that at least 26 drill holes have been completed. Most of these, admittedly, are near the pluton's contact, in the old Mt. Lindsay mine area, and few are near the skarn marble contact. Some, probably, small, areas of cassiterite-bearing skarn occur, for example, near the skarn-granite contact in DDH 35 and in the Mt. Lindsay mine area, but these have extensive stage II amphibole overprints. The reason

the Main Ore zone skarn has not retained extensive areas of stage IA skarn is probably due to the orientation of the skarn relative to the pluton's contact and the subsequent hydrology. In many examples such as at, for example Kara, Tas. (Wolff, 1978); various Whitehorse Cu-Au skarns, Yukon, Canada (Morrison, 1981); many W-skarns in the Bishop District, California (Bateman, 1965) and particularly in the King Island Scheelite skarn (Kwak and Tan, 1981), skarns are developed above troughs or shelves in the granitoid's upper contact. When the pluton's contact is steeply or vertically dipping as at, for example, the Pine Creek deposit, Bishop, Calif., U.S.A. (Bateman, 1965), only a narrow skarn zone occurs, commonly from a few meters wide to 30 metres wide.

The Main Ore zone skarn occurs almost entirely above a shelf in the pluton's surface while the No. 2 skarn occurs along a slightly more steeply dipping contact (Figure 11). The solutions which produced the stage II alteration in the No. 2 skarn extended at least 100 metres out normal to the pluton's contact. As the Main Ore zone skarn (that which is still retained after erosion) extends less than 100 metres from the contact, nearly all of it has reacted to stage II skarn with the loss of much tin, as discussed. The large remnant of stage IA skarn in the No. 2 skarn unit is thus probably due to its orientation relative to the granite's contact. In the Mt. Lindsay skarns, it is unlikely any economic tin stage IA skarns will be found along either steep or above flat granite contacts although the potential for tungsten does exist.

U28

735029

Figure 1

The location of the Mt. Lindsay skarn deposits in Western Tasmania, Australia. The skarns lie stratigraphically above the "Mine Sequence", the host for the huge Renison Tin mine. Minor skarns of various types, including sulphide-rock and magnetite-rich ones also occur in what has been interpretted as the Crimson Creek formation and near the Pine Hill granite. This granite is, in part, a metasomatic - tourmaline - quartz ± topaz ("Luxillianite") rock.

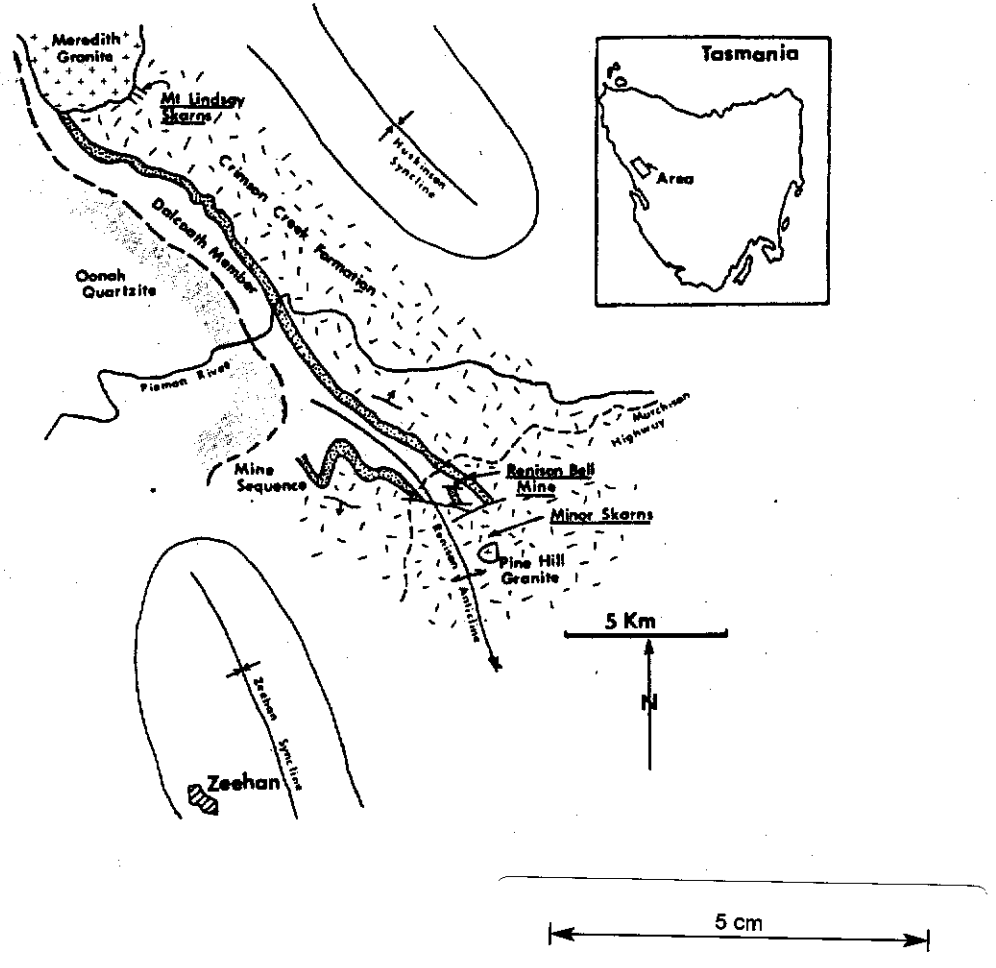
Meredith Granite
Mt Lindsay Skarns
Crimson Creek Formation
Dalcoath Member
Oonah Quartzite
Piemon River
Mine Sequence
Renison Bell Mine
Minor Skarns
Pine Hill Granite
Renison Anticline
Hurtle Highway
Hutchison Syncline
Zeehan Syncline
Zeehan
Tasmania
Area
5 Km
N
5 cm

Figure 2

Plan view of the No. 1, Main Ore Zone and No. 2 skarn units showing their orientation relative to the granites contact. Figure 2 shows contours (in metres) on the granite contact, contours on an interpretted low angle fault and the contact between these two structural features projected up, onto the plan view. The 2000 metre contour is taken as equivalent to sea level. Sections A-B and C-D show the granite contact, fault, and dip of the skarn units (to the southwest). Figure 2B shows the contacts between the skarn and both the interpretted fault and the granite contact. Because of displacement along the fault, skarn-fault contacts exist for upper and lower segments of the skarn units. The sections A-B and C-D best show this feature.

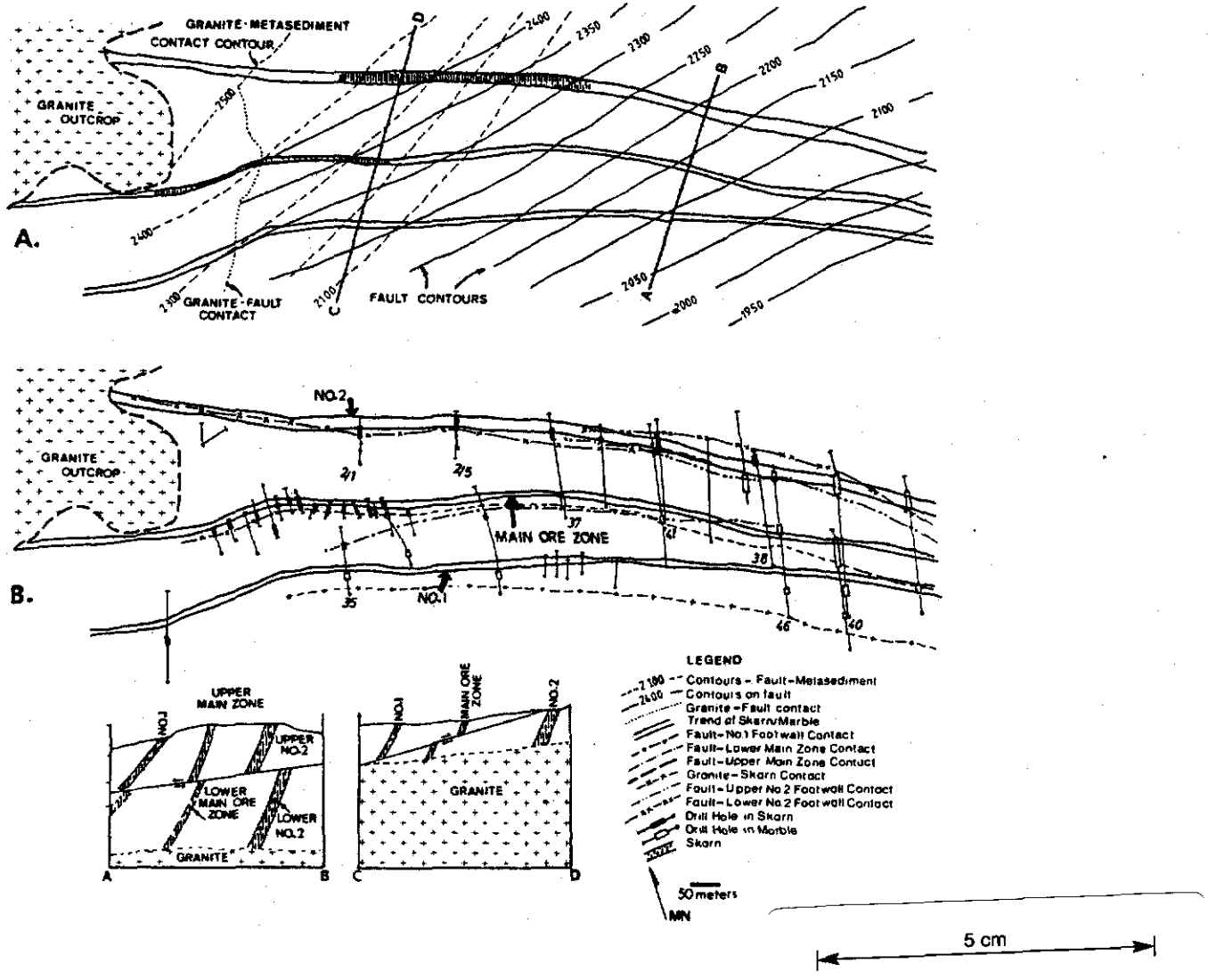
GRANITE-METASEDIMENT CONTACT CONTOUR
GRANITE OUTCROP
A.
GRANITE-FAULT CONTACT
FAULT CONTOURS
B.
NO.2
NO.1
MAIN ORE ZONE
UPPER MAIN ZONE
LOWER MAIN ORE ZONE
UPPER NO.2
LOWER NO.2
GRANITE
LEGEND
Contours - Fault-Metasediment
Contours on fault
Granite-Fault contact
Trend of Skarn/Marble
Fault-No.1 Footwall Contact
Fault-Lower Main Zone Contact
Fault-Upper Main Zone Contact
Granite-Skarn Contact
Fault-Upper No.2 Footwall Contact
Fault-Lower No.2 Footwall Contact
Drill Hole in Skarn
Drill Hole in Marble
Skarn
50 meters
MN
5 cm

Figure 3

A plan of view of the distribution of stage I skarn minerals. The true skarn dimensions are shown in A- while in B- to M- the dimension normal to the skarn contact has been exaggerated relative to the skarn length by a factor of 4:1. This is for ease of representation. A- shows the distribution of "salt and pepper" textural skarn (S + P = Stage IA) and calcsilicate skarn (Ca = Stage IB). This distribution is obvious in drill holes 41, 38 and 46; more interpretative in 2/5, 37 and 47; and impossible to define in 2/1 where stage I mineralogy and pseudomorphic textures have been obliterated.

The dots on the horizontal projections of the drill holes are where the greatest density of samples occur.

C- shows the distribution of magnetite. Area 1 represents an area where magnetite has euhedral or "atoll" type textures (see plate IA) while in area 2 magnetite is massive and anhedral.

D- shows the distribution of ilmenite. In area 1 it occurs as euhedral tabular crystals (plate IE), while in area 2 it occurs as anhedral corroded relicts, often partly altered to Sn-sphene (plate IF).

E- shows the distribution of both F-rich (metasomatic) and F-poor (metamorphic) vesuvianite.

F- shows the distribution of red garnet and pyroxene.

G- shows the distribution of euhedral quartz crystals (area 1) and anhedral quartz interstitial to other minerals (area 2).

H- shows the distribution of fluorite, generally the area equivalent to area 1 of the quartz distribution contains more euhedral fluorite

crystals (cubes) in carbonate.

I- shows the distribution of cassiterite. The stars represent areas where corroded crystals of cassiterite occur (see plates IC and ID).

J- is the distribution of K-feldspar, the stars again represent areas where corroded K-feldspar crystals occur.

K- shows the distribution of siderite ± ankerite. The stars represent areas where radiating "bursts" of siderite occur (see figure IIF).

L- is the distribution of (high Fe) calcite in skarn. That in marble (M) is significantly different in composition (see figure 5).

M- shows the occurrences of danalite (stars) and scheelite (dots).

034

735035

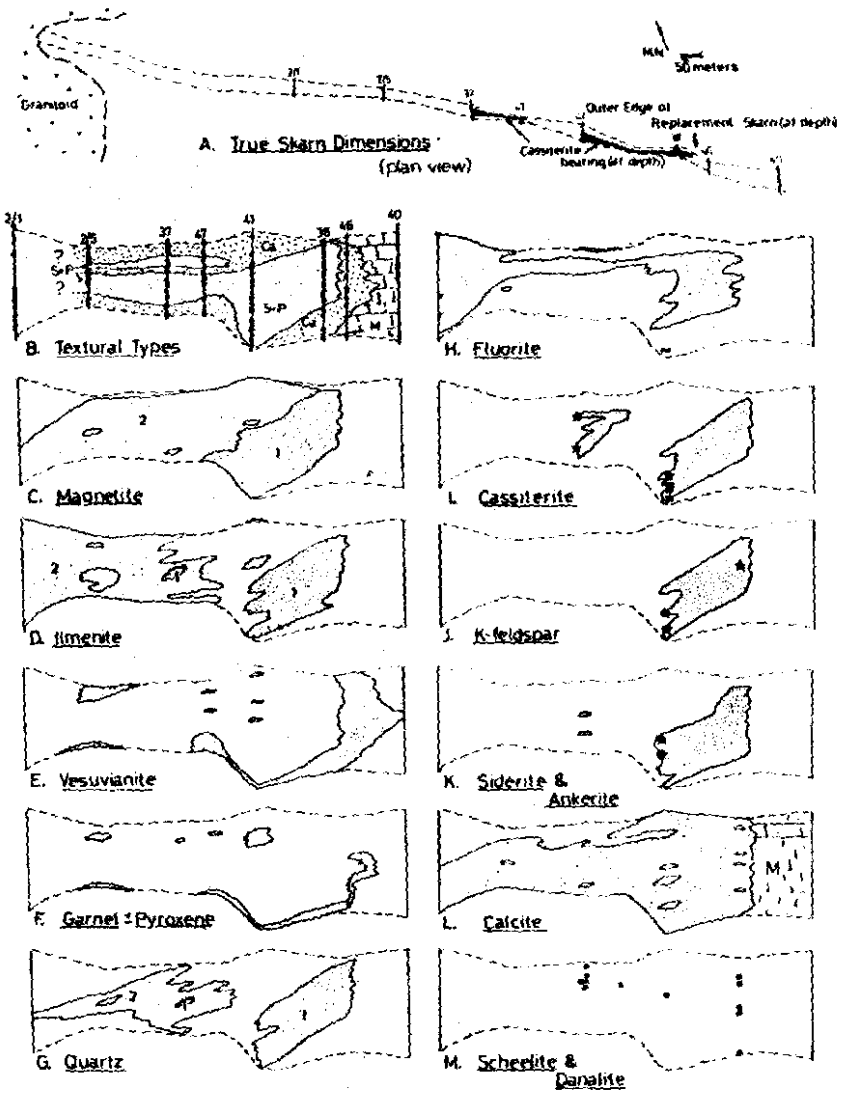
Granitoid
50 meters
Outer Edge of Replacement Skarn (at depth)
Cassiterite bearing (at depth)
A. True Skarn Dimensions (plan view)
B. Textural Types
H. Fluorite
C. Magnetite
I. Cassiterite
D. Ilmenite
J. K-feldspar
E. Vesuvianite
K. Siderite & Ankerite
F. Garnet : Pyroxene
L. Calcite
G. Quartz
M. Scheelite & Danalite
5 cm

Figure 4.

The distribution of stage II and III skarn mineral assemblages.

A- shows the true dimensions of the No. 2 zone skarn and the approximate position of green (not pale) amphibole.

B- this is similar to 3A except that the stage II skarn zones are shown.

C- the distribution of pyrite as a matrix mineral (stipled area) and in veins (solid diamonds).

The letters in the figure refer to the following:
D, arsenopyrite as a matrix mineral; E, ilvaite; F, Sn-sphene, G, chalcopyrite; H, green amphibole (ferrohastingsite); I, pale amphibole (tremolite-actinolite); J, pyrrhotite; K, biotite; L, stilpnomelane and chlorite (mainly) and M, stannite (inverted solid triangles), apophyllite (solid diamonds), sphalerite (solid square), hematite (open square), bismuthinite (solid triangles).

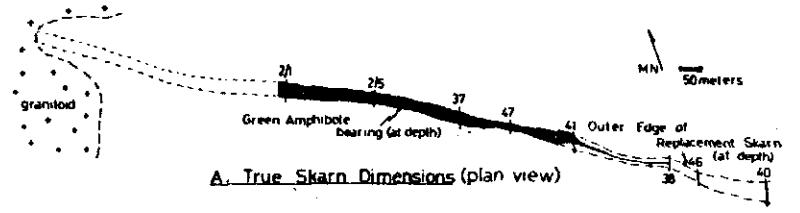

A. True Skarn Dimensions (plan view)

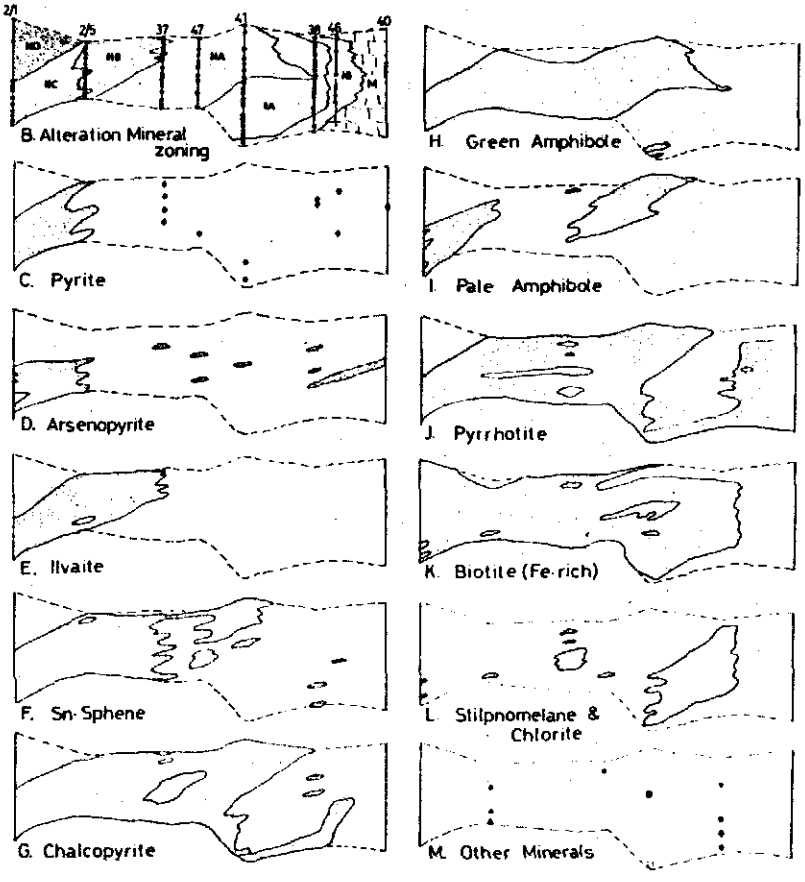

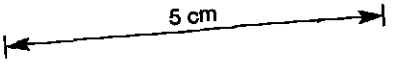

Figure 5

The compositions of carbonates present in the skarns and unreplaced marble. The values are on a molar basis.

A- shows the distribution of coexisting siderite and ankerite in stage IA skarn. The skarn calcite analyses are only a part of the total analyzed.

B- shows skarn calcite (solid squares) and marble calcite analyses (circles).

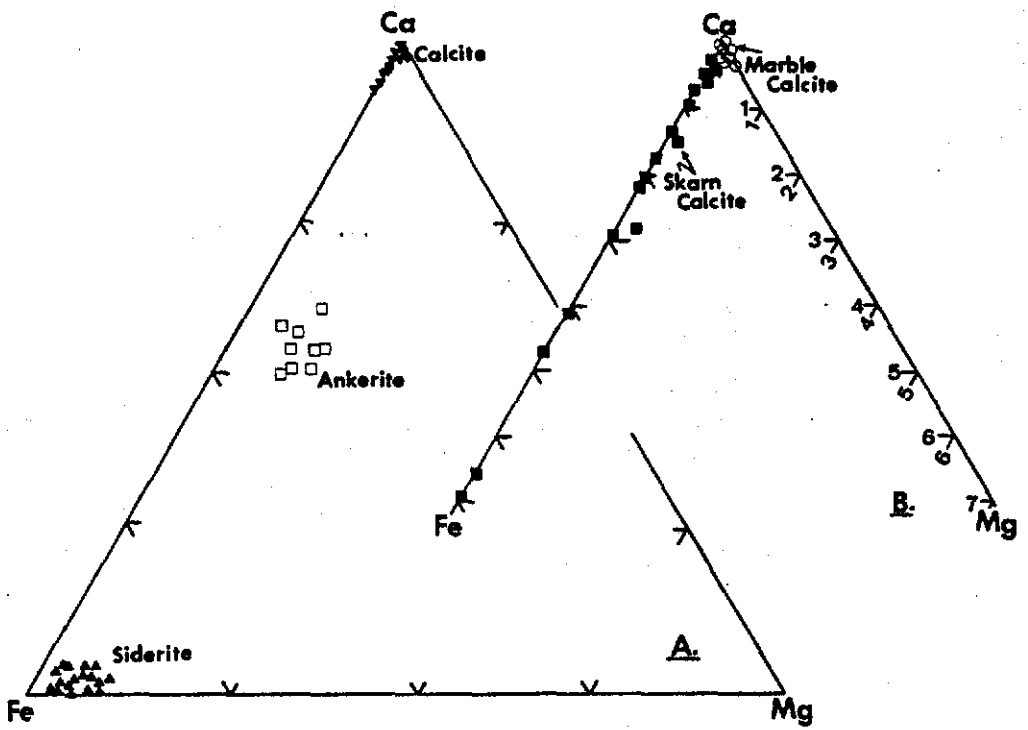
Ca
Calcite
Ankerite
Siderite
Fe
Mg
A.
Ca
Marble Calcite
Skarn Calcite
1
2
3
4
5
6
7
Fe
Mg
B.

Figure 6

Compositions of amphiboles present in stage II skarns.

The diagram is Na + K (molar) vs four fold co-ordinated aluminium ($[Al]^4$) after Deer Howie and Zussman (1962). The ("pale" amphibole) tremolite - actinolite compositions generally post date the ("green" amphibole) ferrohastingsite compositions, the former often forming outer rims (see plate IIE).

040

735041

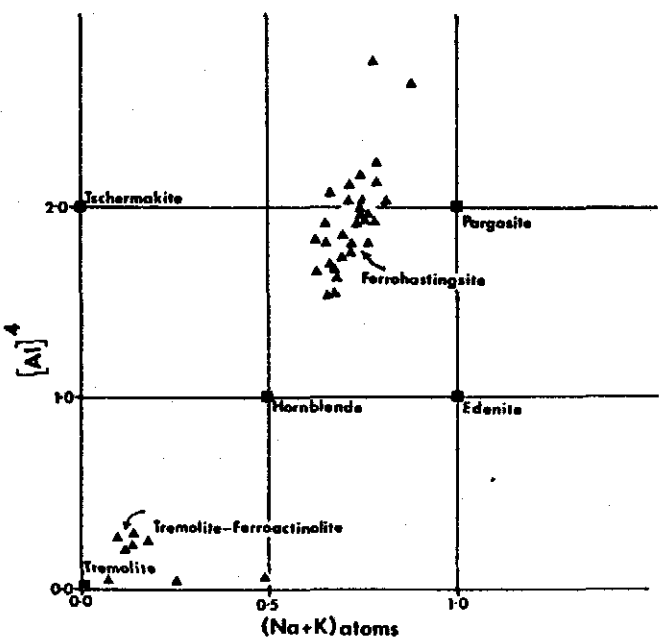
Tschermakite
Pargasite
Ferrohastingsite
Hornblende
Edenite
Tremolite–Ferroactinolite
Tremolite
2·0
1·0
0·0
0·0
0·5
1·0
[Al]^4
(Na+K) atoms

Figure 7

The relation between tin (Sn) content and other compositional parameters in amphibole, garnet + pyroxene + vesuvianite + annite, sphene and ilvaite. In garnet and amphibole an increase in Sn is coincidental with Fe + Mn. Pyroxene, vesuvianite and annite are all very low in Sn. In sphene and ilvaite Sn increases dramatically with increasing Ti. Note that amphibole can have up to 0.78 weight percent Sn.

042

735043

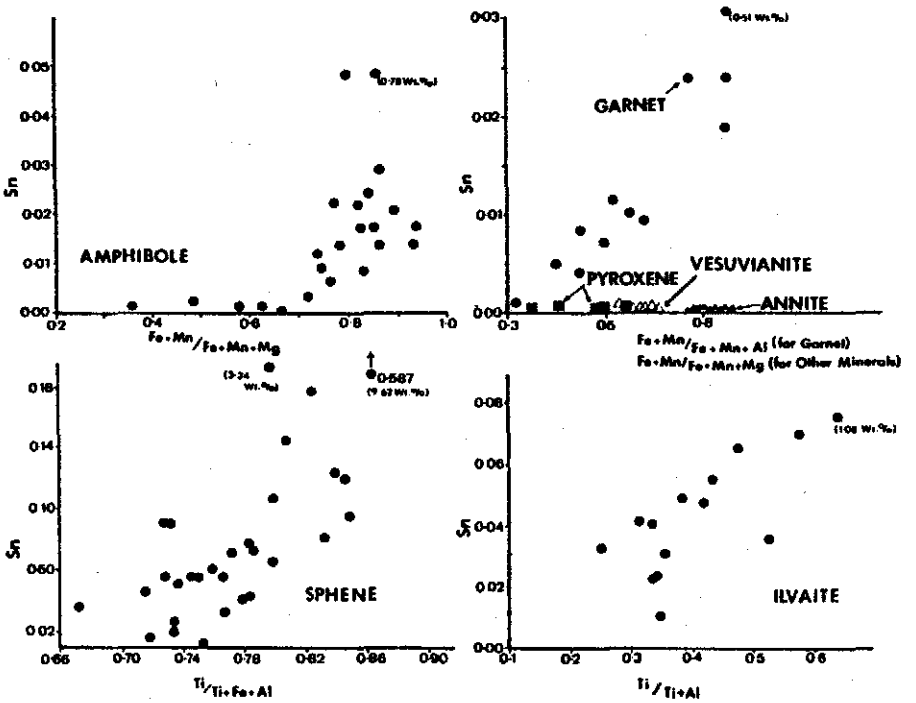
AMPHIBOLE
GARNET
PYROXENE
VESUVIANITE
ANNITE
SPHENE
ILVAITE
Sn
Fe+Mn/Fe+Mn+Mg
Fe+Mn/Fe+Mn+Al (for Garnet)
Fe+Mn/Fe+Mn+Mg (for Other Minerals)
Ti/Ti+Fe+Al
Ti/Ti+Al

Figure 8

Orientation of zonation in the skarn. Most of the mineral distribution patterns shown in figures 3 and 4 are similar to the plan view shown here (8-3). The drill holes were oriented from the south west (collar) towards the north east (see figure 2). The distribution pattern (figure 8-3) can only be explained if the plane of the minerals' "out isograd" relative to the granites contact, slopes towards the east. This would have to be almost co-planar to the granite contact. As the angle of intersection ("α" in figure 8-3) of the minerals' "out" and "in" isograds with the margins of the skarn are very similar (see figures 3 and 4). The zonation must be very systematic as shown in figure 11.

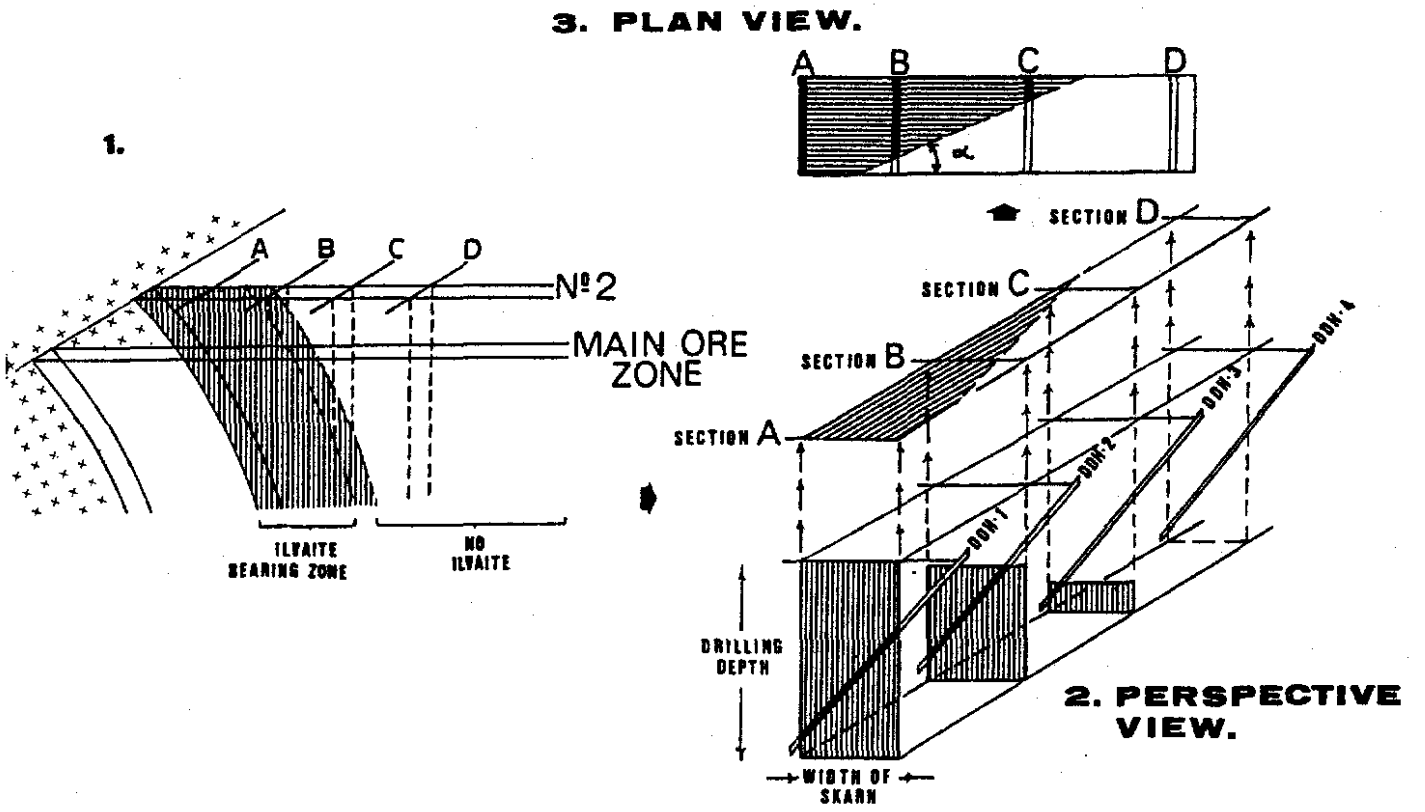
3. PLAN VIEW.
A
B
C
D
α
1.
A
B
C
D
Nº2
MAIN ORE ZONE
ILVAITE BEARING ZONE
NO ILVAITE
SECTION D
SECTION C
SECTION B
SECTION A
DDH-4
DDH-3
DDH-2
DDH-1
DRILLING DEPTH
WIDTH OF SKARN
2. PERSPECTIVE VIEW.

Figure 9

The distribution of W, Sn, Ag and Cu in the skarns taken as an average of the skarn intersections in each drill hole.

A. Sn_{Total} and $Sn_{acid\ soluble}$ values. The ranges and number of analyses represented by the bars are as follows: DDH 2/1 range of Sn_{Total} = 0.21 - <0.01, range of $Sn_{acid\ soluble}$ = Not determined (N.D.), number of analyses = 16; DDH 2/5, 0.17 - 0.07, N.D., 10; DDH 37, 0.24 - 0.01, 0.131 - 0.011, 35; DDH 47, 0.38 - 0.01, 0.140 - 0.025, 28; DDH 41, 0.58 - 0.07, 0.170 - 0.011, 54; DDH 38, 2.35 - 0.01, 0.015 - <0.003, 25; DDH 46, 0.05 - <0.01, 0.042 - 0.011, 20.

B. Tungsten values. As for Sn_{Total} + $Sn_{acid\ soluble}$, DDH 2/1, range = 0.02 - <0.01, 16 analyses; DDH 2/5, 0.02 - <0.01, 10; DDH 37, 0.32 - <0.01, 35; DDH 47, 0.14 - <0.01; DDH 41, 0.09 - <0.01, 54; DDH 38, 0.16 - <0.01, 25; and DDH 46, <0.01, 20.

C. Copper values. As for Sn_{Total} + $Sn_{acid\ soluble}$. DDH 2/1, 0.07 - <0.01, 16; DDH 2/5, 0.15 - 0.04, 35; DDH 37, 0.40 - <0.01, 35; DDH 47, 0.20 - <0.05, 28; DDH 41, 0.28 - 0.07, 54; DDH 38, 0.81 - <0.05, 25, and DDH 46, <0.05, 20.

D. Arsenic values. As for Sn_{Total} + $Sn_{acid\ soluble}$. DDH 2/1, 0.20 - <0.01, 16; DDH 2/5, 0.32 - 0.01, 35; DDH 37, 0.92 - <0.01, 35; DDH 47, <0.10, 28; DDH 41, <0.10, 54; DDH 38, 1.42 - <0.01, 25; and DDH 46, <0.10, 20.

In addition, the following values of other elements occur for the following drill holes: DDH 37, Bi = 0.02 (average), 0.22 - <0.01 range, 35 samples; Mo, <0.01, 0.02 - <0.001, 35; Zn, 0.15, 0.24 - 0.11, 15; Fe_{Total}, 37.9, 54.2 - 13.4, 35; Pb, 0.003, 0.012 - 0.002, 15; S, 1.872, 3.05 - 0.24, 15. ML 47, Bi, 0.010 average, 0.044 - 0.004 range, 28 samples; Zn, 0.013, 0.030 - 0.007, 28; Fe_{Total}, 33.6, 53.0 - 11.9, 28; Pb, 0.003, 0.006 - 0.001, 28; Ag, 4ppm, 5 - 2 ppm, 28. DDH 41; Bi, 0.008, 0.025 - 0.005, 24; Fe_{Total} 35.4, 56.8 - 9.9, 54. DDH 38; Bi, 0.20, 0.062 - 0.004, 25; Mo, 0.001, 0.002 - 0.001, 25; Fe_{Total}, 29.5, 39.3 - 16.2, 25; S, 1.55, 4.42 - 0.21, 25; Ag, 2.8ppm, 7.9 - 0.1, 4; Au, 0.005ppm, 0.010 - 0.00ppm, 4. ML 46, Bi, 0.010, 0.026 - 0.006, 20; Zn, 0.010, 0.016 - 0.005, 20; Fe_{Total}, 6.50, 13.5 - 4.2, 20; Ag, 7ppm, 9 - 5ppm, 20; Pb, 0.006, 0.008 - 0.004, 20.

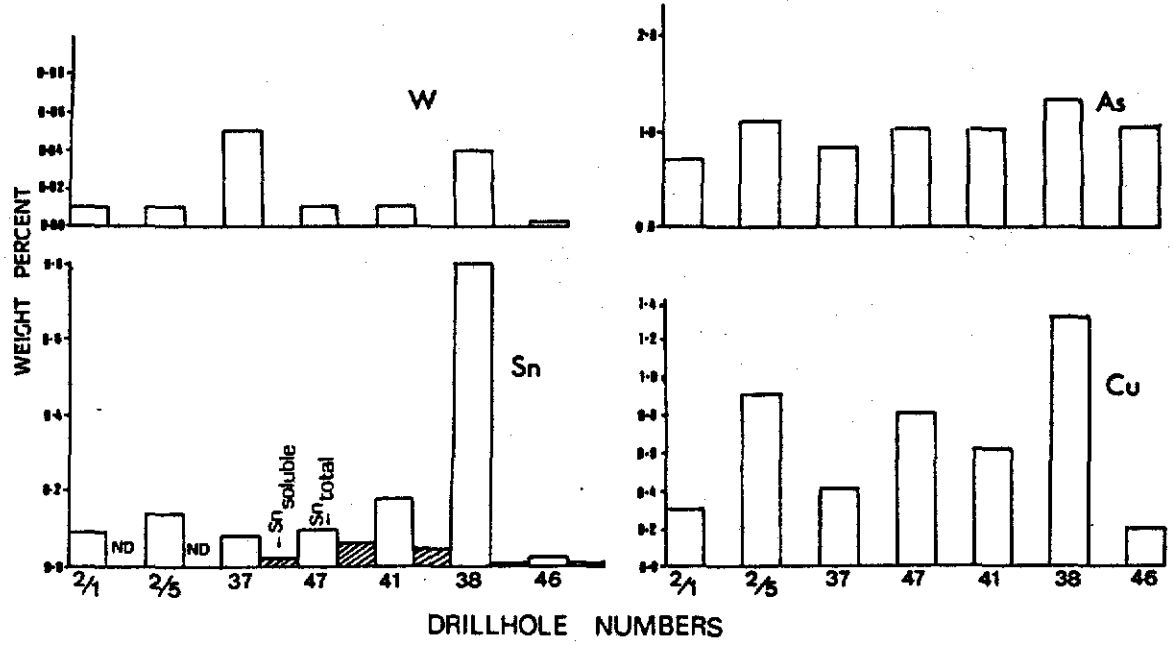
W
As
Sn
Cu
WEIGHT PERCENT
ND
ND
Sn soluble
Sn total
2/1
2/5
37
47
41
38
46
DRILLHOLE NUMBERS

Figure 10

Approximations of conditions present during skarn genesis.

A- Temperatures vs log f_{O_2} diagram of coexisting magnetite-ulvospinel vs ilmenite - hematite pairs after Linsley, 1963. The solid lines represent those after Linsley while the dashed lines are extensions of these done in the present study. The points are derived from analysis of coexisting $ilmenite_{ss}$ - $magnetite_{ss}$ pairs. The numbers refer to drill hole numbers (see figure 2). In each case between 5 and 10 pairs were analysed.

B- Log f_{S_2} vs log f_{O_2} relations after Sato, 1980 (his figure 10) at 400°C. Conditions in stage I skarn must be near the lower solid square (1); that in stage IIA and B, near 2; and that in IIC and D near 3. Abbreviations: Fe, iron; Mt, magnetite; Po, pyrrhotite; Py, pyrite; Hem, hematite; And, andradite; Qtz, quartz; Hd, hedenbergite.

C- log f_{O_2} - temperature plot showing $biotite_{ss}$ compositions after Wones and Eugster, 1965. The biotites in the present study plot near Fe/Fe + Mg = 90. New abbreviations: San, sanidine; G, gas.

D- Log f_{O_2} vs temperature diagram of various buffer curves after Sato, 1980 (his figure 9). Superimposed upon this is the data of French, 1971. Lines (a), (b) and (c) are for the total pressures of 2000, 1000 and 500 bars. Conditions during stage IA skarn crystallization must have been <u>below</u> the And-Qtz-Mt buffer at temperatures in the range of 400 to 450°C. This gives an f_{O_2} of near 10^{-27} which is consistent with that in 10A for the same skarn stage. Abbreviations: Sid, siderite; Gr, graphite; No, nickel oxide; N, nickel and Fa, fayalite.

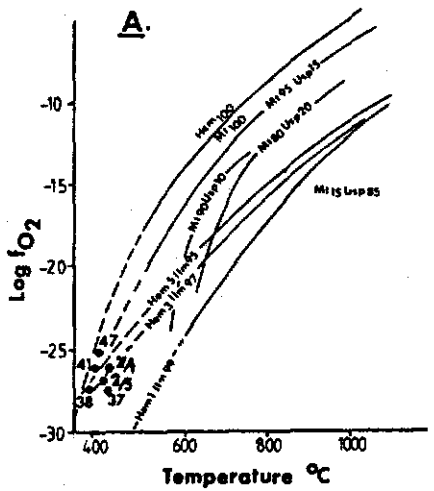
A.
Log f_{O_2}
Temperature °C
-10
-15
-20
-25
-30
400
600
800
1000

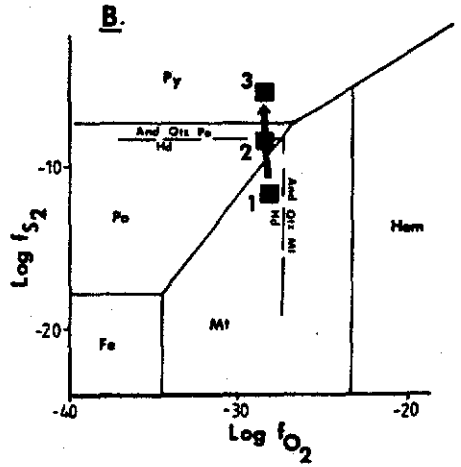
B.
Py
Po
Fe
Mt
Hem
Log f_{S_2}
Log f_{O_2}
-10
-20
-40
-30
-20

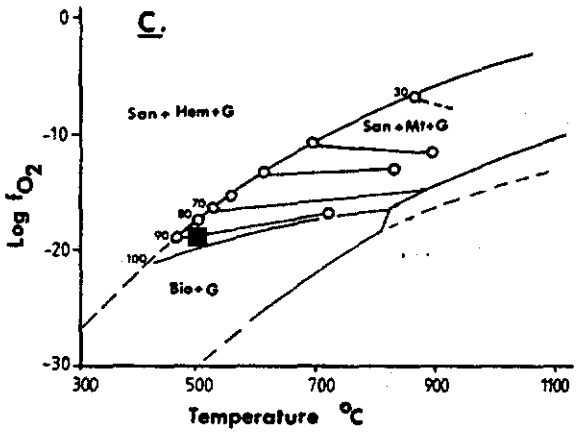
C.
San + Hem + G
San + Mt + G
Bio + G
Log f_{O_2}
Temperature °C
0
-10
-20
-30
300
500
700
900
1100

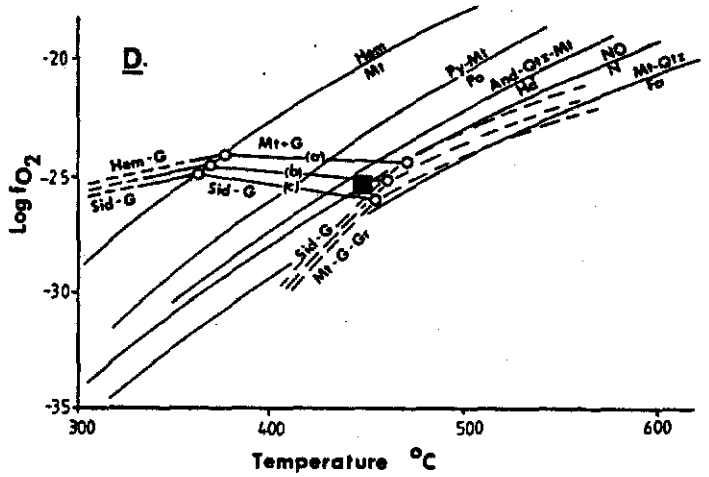
D.
Hem
Mt
Py-Mt
Po
And-Qtz-Mt
Hd
NO
Mt-Qtz
Fa
Mt + G
Hem - G
Sid - G
Log f_{O_2}
Temperature °C
-20
-25
-30
-35
300
400
500
600

Figure 11

The zoning and distribution of drill holes in the No. 2 (A) and Main Ore zone (B) skarns.

The interpretted zonation in the upper No. 2 skarn zone. The zonation is determined from a section taken very near the southwest contact of the No. 2 skarn. The distribution of minerals is derived from figures 3 and 4 with figure 2. The angle between the skarn zones are partly interpretive as is the extent of "subgreisen" (see text). The drill hole numbers 37, 38, 40 and 46 are repeated in the No. 2 and Main Ore zone because the drill holes were inclined and intersected both units. The skarn stages IA to IID are described in the text.

An, annite; Fl, fluorite; Ga, green amphibole; PA, pale amphibole; IV, ilvaite; MG, magnetite; Po, pyrrhotite; AS, arsenopyrite; SP, sphene; CP, chalcopyrite; PY, pyrite; SI, siderite; CA, cassiterite; KF, K-feldspar; Il, ilmenite; TG, titanium-rich garnet; FV, fluorine-rich vesuvianite. The distributions refer to matrix minerals, not ones in veins. The underlined symbols represent "out" isograds meaning this mineral does not occur farther out from the granite contact while the non-underlined ones represent "in" isograds, meaning where the mineral first appears, and from the granite contact. The zonal pattern would be only slightly different if some other longitudinal section had been chosen.

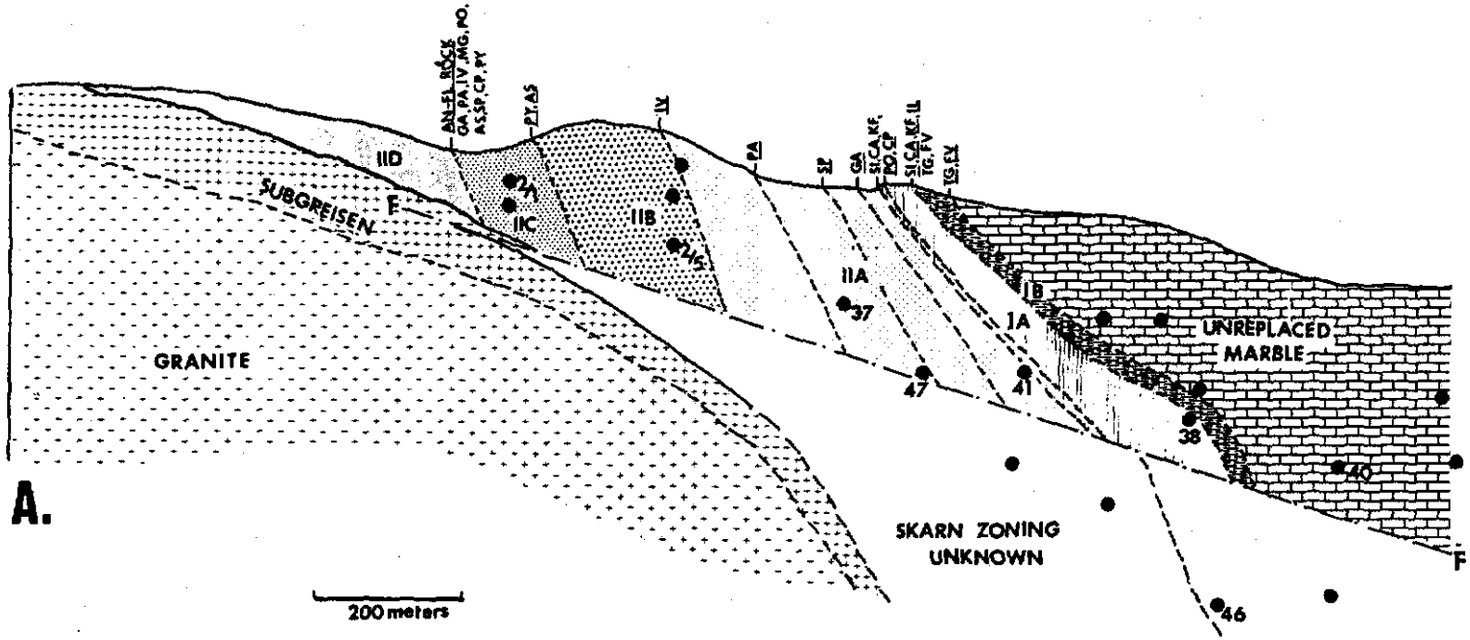
AN-EL ROCK
QA, PA, IV, MG, HO,
AS, SP, CP, PY
PY, AS
IV
PA
SP
QA
SI, CA, KF,
EO, CP
SI, QA, KF, IL
TG, FV
TG, EV
IID
IIC
IIB
IIA
IB
1A
SUBGREISEN
F
GRANITE
UNREPLACED
MARBLE
SKARN ZONING
UNKNOWN
37
47
41
38
40
46
F
200 meters

A.

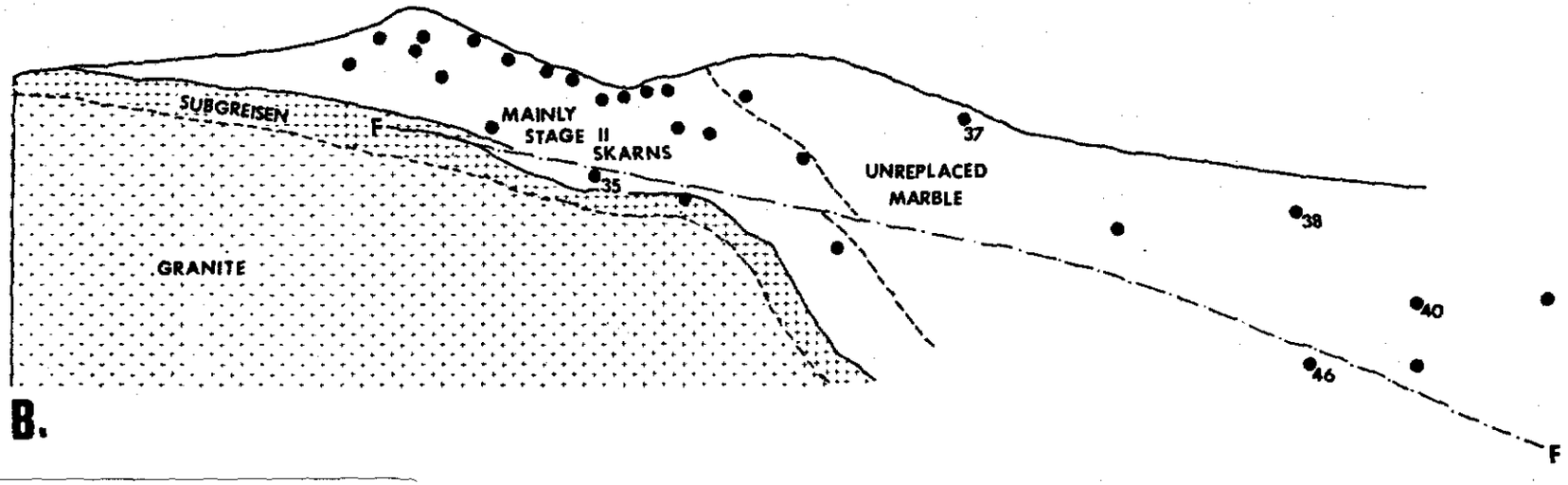
SUBGREISEN
F
MAINLY
STAGE II
SKARNS
35
37
UNREPLACED
MARBLE
38
40
46
F
GRANITE

B.

5 cm

Figure 12

Solubilities of Sn in terms of log f_{O_2}, pH, ionic strength and temperature (after Eadington and Giblin, 1979).

A- shows iso-solubility lines of Sn in pH vs log f_{O_2} space. This relationship is for 400°C, $a_{Cl^-} = 1$, a_{F^-} is controlled by fluorite. The contours are the sum of the activities of the $SnCl_2^0(aq)$ and $SnF^+(aq)$ complexes. The stipled area represents the probable pH and f_{O_2} of hydrothermal solutions (according to Eadington and Giblin). These occur near the muscovite-K-feldspar (pH) buffer. If such a solution at (1) is neutralized by reaction with carbonate, conditions at (2) would occur and essentially all Sn would precipitate. Later, low pH solutions could redissolve Sn if the buffer system is no more present (i.e. all calcite consumed) and if this solution were undersaturated with Sn under these conditions (see text).

B- the same relationships hold here as in (A) except that the temperature is now 250°C. Clearly, a decrease of temperature from 400°C to 250°C would precipitate essentially all the Sn as well.

C- the position of the 10^{-3} (112 ppm Sn) contour for $SnCl_2^0(aq)$, the principal tin complex, is shown at activities of Cl^- from 0.01 to 10 molal. Temperature = 500°C.

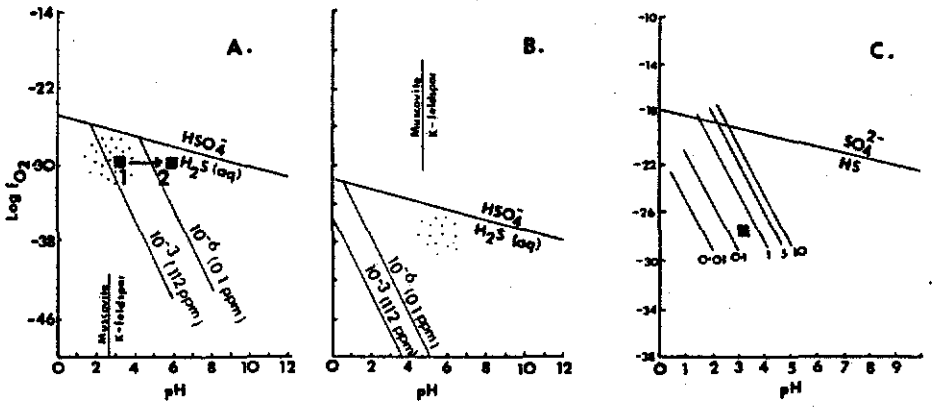
A.
B.
C.
Log f_{O_2}
pH
HSO_4^-
H_2S (aq)
SO_4^{2-}
HS^-
10^{-3} (112 ppm)
10^{-6} (0.1 ppm)
Muscovite
K-feldspar
0·01
0·1
1
5
10

Table 1.

Bulk chemical analyses of the granite below the skarns (done at La Trobe University) and skarns (after Kinealy, 1979). In the granites, the samples come from drill hole 35 (see figure 2), just below the skarns. The depths are 1 = 255 metres; 2 = 262 metres; 3 = 264.5 metres; 4 = 266.5 metres; 5 = 274.8 metres, 6 = 277.3 metres and 7 = 279.6 metres. Skarn occurs at approximately -254 metres. The major oxides SiO_2, TiO_2, Al_2O_3, Fe_{Total}, MnO, MgO, CaO, P_2O_5 and SO_3 were analyzed by X-ray spectroscopy; K_2O and Na_2O by flame photometry; H_2O and CO_2 by weight difference on absorption of phosphorus pent oxide and "carbsorb" respectively; FeO by colorimetry.

The lower values of the granite (/subgreisen) samples nearest the skarn are probably due to the fact that fluorine was not analyzed for.

The skarn sample numbers in Kinealy's report with drill hole (ML) numbers and depths in metres are as follows: 8 = 64262, DH2/1, -79.6 metres; 9 = 64263, ML 2/1, -91.1 m; 10 = 64261, Ml = 2/1, -72.9 m; 11 = 64260, JL 2/1, 65.2 m; 12 = 64267, ML 47, -300.16 m; 13 = 64268, ML 47, -307.8 m; 14 = 64279, ML 38, -759.1 m; 15 = 64282, ML 38, -363.4 m; 16 = ML 38, -339.8 m; 17 = 64264, ML 2/3, -50.1 m.

Major elements including sulphur were analyzed by X-ray fluorescence after lithium borate fusion. Sodium was done by atomic absorption, fluorine by specific ion electrode and ferrous iron by dichomate titration. H_2O^+, H_2O^- and CO_2 were determined gravimetrically. Tin was analyzed by X-ray fluorescence (Sn < Kα, 3.560Å) in a pressed powder disc and separately by amminium iodide volatilization and atomic absorption. Using the ammunium iodide technique tin in the lattice of non-reactive minerals will not be detected. Tin analyses using X-ray fluorescnece suffers from Ca, K α (3.359 Å) and K, K α (3.742Å) interference. Overlap corrections were made for this, but are not accurate for these samples containing high Ca (> 20%).

Sample No.:	GRANITE SAMPLES 1	2	3	4	5	6	7	SKARN SAMPLES 8	9	10	11	12	13	14	15	16	17
SiO_2	74.89	76.27	75.45	75.86	74.95	74.95	75.24	38.12	23.86	13.57	37.49	11.50	13.72	14.68	11.93	40.30	15.12
TiO_2	0.07	0.09	0.10	0.09	0.10	0.10	0.09	0.73	1.37	0.85	0.99	0.97	0.39	1.07	0.78	2.28	0.38
Al_2O_3	11.92	11.91	11.73	12.18	12.26	12.59	12.63	9.35	10.74	5.38	9.28	6.14	2.82	5.65	15.74	7.90	6.05
Fe_2O_3	0.00	0.39	0.00	0.01	0.04	0.00	0.00	4.93	4.75	36.22	4.48	35.08	35.21	15.76	12.43	-*	3.26
FeO	1.19	0.89	1.57	1.31	1.41	1.69	1.05	18.40	17.80	26.40	22.90	25.20	25.10	28.90	35.80	9.04	3.90
MnO	0.03	0.02	0.02	0.03	0.03	0.04	0.02	0.19	0.22	0.38	0.52	0.28	0.32	0.26	0.65	0.37	0.53
MgO	1.07	0.39	0.35	0.30	0.22	0.20	0.35	1.94	2.68	2.35	5.03	1.65	2.35	1.59	1.79	7.07	1.58
CaO	0.86	0.76	0.56	0.69	0.78	0.74	0.89	8.84	18.47	5.36	11.34	5.15	7.39	2.67	1.34	20.02	40.35
Na_2O	2.50	2.40	2.85	3.07	2.93	3.01	3.35	0.24	0.26	0.48	0.95	0.39	0.08	0.04	0.03	0.83	0.11
K_2O	5.37	5.03	5.09	5.11	5.28	5.16	5.53	4.10	4.32	0.45	0.88	0.55	0.20	2.29	2.81	0.44	0.09
P_2O_5	0.05	0.05	0.05	0.04	0.06	0.05	0.05	0.67	0.67	0.36	0.49	0.31	0.35	0.39	0.27	0.74	1.59
H_2O^+	0.70	0.64	0.79	0.61	0.89	0.76	0.40	1.77	3.43	0.70	1.80	0.73	1.19	1.88	1.19	1.48	0.51
H_2O^-	0.15	0.11	0.13	0.10	0.10	0.13	0.07	1.67	1.18	1.28	1.40	1.01	0.75	1.49	0.20	0.72	0.82
CO_2	0.63	0.49	0.33	0.26	0.48	0.62	0.53	0.39	0.28	0.29	0.47	7.19	9.52	22.53	12.62	0.00	23.90
S	0.02	0.02	0.01	0.04	0.02	0.04	0.04	0.11	0.02	1.37	0.08	0.20	0.08	0.08	0.01	8.36	0.12
F								10.2	13.10	0.24	0.41	0.19	0.11	0.42	0.26	0.31	0.31
Total	99.43	99.47	99.04	99.70	99.55	100.07	100.24	101.31	103.15	95.68	98.51	96.54	99.58	99.69	99.94	99.86	98.71
-S≡O	0.01	0.01	0.01	0.02	0.01	0.02	0.02	.06	0.01	0.68	0.04	0.10	0.04	0.04	0.00	0.00	0.06
-O≡F								4.29	5.52	0.10	0.17	0.08	0.05	0.18	0.11	0.13	0.13
TOTAL	99.42	99.46	99.03	99.68	99.54	100.05	100.22	96.96	97.66	94.98	98.30	96.36	99.49	99.47	99.83	99.73	98.52
Sn(ppm) by X.R.F.								13	21	1018	1328	1095	241	13,249	365	4.85	163
Sn(ppm) by volatilization method								130	100	750	560	760	240	21,200	430	1.90	<100

Table 2

The compositions of hydrous minerals present in granite and skarn. For this and subsequent tables chemical compositions were determined by means of a Joel JXA-5A electron microprobe with computer control, located at the Department of Geology, University of Melbourne using a beam current of 0.1 mA and an accelerating potential of 15 kV. The following standards were used: SiO_2 wollastonite and quartz; Al_2O_3 corundum; TiO_2, rutile; Fe total and Ba, anandite; K_2O, potassium tantalite; Mn metal; Ni, Ni metal; F, fluorite; Cl, halite; Sn, Sn metal; W, W metal; Zn, Zn metal; Cu, Cu metal; and Na, jadeite. The computer program for the reduction of electron microprobe data was written by Mason et al. (1969) with modifications by A.K. Ferguson.

Biotite members D-17, comes from the granite in drill hole ML35, D-17 and D7-5 are phengites from ML-35. Biotites D7-99 and D8-78 are from ML37 and D7-68, from ML2-1. The chlorites are from ML-2/5 (D8-6), ML38 (D7041) and ML41 (8-29) stilpnomelane is from ML2-1 and apophyllite, from ML38.

	Biotite + phengite							Chlorite				Stilpnomelane	Apophyllite
Sample No.:	D7-17	D7-17	D7-5	D7-99	D7-66	D7-68	D8-7a	D8-7b	D8-6	D7-41	D8-29	D7-66	D7-32
SiO_2	33.01	49.12	51.67	36.31	33.86	33.53	34.56	35.21	25.77	23.30	25.22	59.24	50.79
TiO_2	2.84	0.03	0.07	0.81	1.13	0.69	0.30	1.04	0.01	0.05	0.04	0.01	0.00
Al_2O_3	15.55	34.00	35.88	11.08	13.32	13.68	11.57	11.68	14.77	19.00	15.92	0.70	0.17
FeO	30.97	3.96	2.26	27.63	34.54	32.57	35.99	35.59	43.82	41.69	42.67	24.73	0.00
MnO	0.22	0.09	0.05	0.35	0.29	0.25	0.25	0.22	0.60	0.01	0.08	0.71	0.03
MgO	2.80	0.23	0.50	7.76	1.94	3.51	2.70	3.35	3.38	2.92	3.07	2.03	0.01
ZnO	0.06	0.01	0.05	0.09	0.08	0.08	ND	0.05	0.03	0.05	0.05	0.03	0.07
CuO	0.06	0.07	0.05	0.05	0.00	0.00	ND	ND	0.01	0.03	0.06	0.05	0.00
SnO_2	0.00	0.02	0.00	0.00	0.02	0.01	0.14	0.02	0.02	0.01	0.00	0.03	0.02
WO_3	0.03	0.00	0.00	0.00	0.00	0.06	0.00	0.05	0.00	0.03	0.10	0.07	0.08
CaO	0.00	0.00	0.00	0.00	0.00	0.00	0.00	0.00	0.16	0.05	0.04	0.44	24.32
Na_2O	0.14	0.07	0.00	0.16	0.30	0.55	0.09	0.08	0.06	0.09	0.10	0.47	0.17
K_2O	8.90	8.86	7.47	8.64	8.31	8.10	8.67	9.15	0.14	0.05	0.14	0.04	4.45
Cl	0.60	0.02	0.01	0.81	1.26	1.01	1.20	0.74	0.03	0.05	0.04	0.03	0.01
F	2.11	1.03	0.61	1.56	0.93	1.97	0.76	0.89	0.00	0.19	0.01	0.28	2.50
Total	96.79	96.50	96.81	95.25	96.01	96.01	96.23	98.13	88.80	87.63	87.53	88.85	92.71
Inferred OH	3.21	3.50	1.39	4.75	3.99	3.99	3.87	1.87	11.20	12.37	12.47	11.15	17.29
	No. of ions on the basis of 24 oxygens							No. of ions on the basis of 36 (O, OH)				No. of ions on the basis of 85	No. of ions on the basis of 28 oxygens
Si	5.336	6.606	6.878	5.654	5.516	5.886	5.608	5.862	5.803	5.119	5.556	Si 8.000	Si 7.104 7.132
Al	2.664 8.000	1.394 8.000	1.122 8.000	2.034 7.688	2.484 8.000	0.944 6.830	2.213 7.821	2.138	2.197 8.000	2.881 8.000	2.443 8.000	Ti 0.001	Al 0.028
Al	0.300	3.996	4.508	0.000	0.074	0.000	0.000	0.154	3.852	2.041	1.690	Al 0.111	Al 0.000
Ti	0.345	0.003	0.007	0.095	0.139	0.091	0.037	0.130	0.004	0.008	0.003	Fe 2.793	Ti 0.000
Fe^{2+}	4.120	0.445	0.252	3.599	4.706	4.782	4.884	4.955	8.253	7.660	7.860	Mn 0.081	Fe^{2+} 0.000
Mn	0.030	0.011	0.006	0.046	0.040	0.037	0.034	0.031	0.115	0.001	0.014	Mg 0.408	Mn 0.003
Mg	0.674 5.485	0.046 4.525	0.099 4.782	1.801 5.557	0.471 5.440	0.919 5.844	0.653 5.618	0.831 6.111	1.134 13.366	0.959 10.689	1.007 10.600	Zn 0.004	Mg 0.001
Zn	0.007	0.001	0.005	0.010	0.010	0.011	ND	0.005	0.005	0.007	0.007	Cu 0.004	Zn 0.007 3.661
Cu	0.008	0.002	0.005	0.000	0.000	0.000	ND	ND	0.001	0.005	0.009	Sn 0.005 3.792	Cu 0.000
Sn	0.000	0.007	0.000	0.000	0.001	0.001	0.010	0.000	0.001	0.001	0.000	W 0.003	Sn 0.000
W	0.001	0.000	0.000	0.000	0.000	0.003	0.000	0.005	0.000	0.002	0.006	Ca 0.063	W 0.003
Ca	0.000	0.000	0.000	0.000	0.000	0.000	0.000	0.000	0.038	0.011	0.009	Na 0.123	Ca 3.644
Na	0.045 1.881	0.017 1.54	0.000 1.268	0.049 0.907	0.094 1.821	1.188 2.002	0.028 1.823	0.026 1.969	0.027 0.106	0.039 0.064	0.042 0.091	K 0.003	Na 0.045
K	1.836	1.520	1.268	0.858	1.727	1.814	1.795	1.943	0.041	0.013	0.039	Cl 0.006	K 0.810 1.964
Cl	0.274	0.004	0.002	0.213	0.348	0.301	0.330	0.208	0.011	0.018	0.014	F 0.119	Cl 0.002
F	1.079 3.085	0.438 1.63	0.257 0.913	0.768 3.596	0.479 3.125	1.094 3.871	0.390 2.888	0.468 1.876	8.926	0.132 9.757	0.006 9.731	(OH) 4.000	F 1.106
OH	1.732	1.188	0.634	2.615	2.298	2.476	2.168	1.100	8.915	9.606	9.710	(O,OH,H_2O) 21.040	OH 8.552

Table 3

Electron microprobe analyses of primary stage IA minerals. The scheelite, rutile and K-feldspar come from drill hole ML38. Cassiterite comes from ML38 (D7-89) and ML47 (the others). Ilmenite-magnetite pairs come from ML38 (D7-38), ML 2/1 (D7-62) and ML41 (D8-18).

Cassiterite

Sample No.:	D8-20	D7-89	D8-19	D8-30
SiO_2	0.00	0.00	0.00	0.00
TiO_2	0.90	0.17	0.47	0.08
Al_2O_3	0.00	0.03	0.00	0.00
FeO	0.24	0.18	0.31	1.38
MnO	0.00	0.04	0.00	0.00
MgO	0.00	0.00	0.00	0.00
ZnO	0.09	0.01	0.00	0.00
CuO	0.09	0.04	0.00	0.06
SnO_2	97.72	98.24	98.39	98.02
WO_3	0.22	0.24	0.06	0.00
CaO	0.00	0.00	0.00	0.00
Na_2O	0.04	0.04	0.06	0.00
K_2O	0.00	0.00	0.00	0.00
Cl	0.01	0.01	0.00	0.01
F	0.70	1.03	0.78	0.57
Total	100.01	100.11	100.07	100.12

No. of ions on the basis of 2 oxygens

Si	0.000	0.000	0.000	0.000
Al	0.000	0.001	0.000	0.000
Ti	0.015	0.003	0.009	0.002
Fe	0.004	0.004	0.006	0.029
Mn	0.000	0.001	0.000	0.000
Mg	0.000	0.000	0.000	0.000
Zn	0.002	0.000	0.000	0.000
Cu	0.002	0.001	0.000	0.001
Sn	0.967	0.971	0.972	0.972
W	0.001	0.002	0.000	0.000
Ca	0.000	0.000	0.000	0.000
Na	0.001	0.002	0.003	0.000
K	0.000	0.000	0.000	0.000
Cl	0.000	0.000	0.000	0.000
F	0.049	0.080	0.061	0.045

K-feldspar

	D7-42	D8-25	D7-28
SiO_2	65.41	65.90	65.04
TiO_2	0.02	0.01	0.01
Al_2O_3	18.28	17.87	18.07
FeO	0.13	0.42	0.89
MnO	0.00	0.04	0.00
MgO	0.01	0.02	0.01
ZnO	0.00	0.02	0.04
CuO	0.06	0.00	0.01
SnO_2	0.00	0.00	0.00
WO_3	0.12	0.06	0.00
CaO	0.00	0.00	0.00
Na_2O	0.13	0.14	0.07
K_2O	15.48	15.69	15.99
Cl	0.00	0.00	0.00
F	0.00	0.07	0.45
Total	99.63	100.22	100.59

No. of ions on the basis of 32 oxygens

Si	12.074	12.102	11.974
Al	3.977	3.868	3.921
Ti	0.003	0.014	0.002
Fe^{+2}	0.020	0.064	0.137
Mn	0.000	0.007	0.000
Mg	0.002	0.006	0.002
Zn	0.000	0.002	0.006
Cu	0.009	0.000	0.001
Sn	0.000	0.000	0.000
W	0.002	0.001	0.000
Ca	0.000	0.000	0.000
Na	0.047	0.051	0.024
K	3.644	3.680	3.754
Cl	0.000	0.000	0.000
F	0.000	0.041	0.262
Mole %	Or 98.7	87.86	99.36
	Ab 1.3	12.14	0.64
	An 0	0	0

Rutile

	D8-25
SiO_2	0.00
TiO_2	97.22
Al_2O_3	0.01
FeO	0.58
MnO	0.00
MgO	0.03
ZnO	0.04
CuO	0.00
SnO_2	0.02
WO_3	0.21
CaO	0.02
Na_2O	0.07
K_2O	0.00
Cl	0.00
F	0.00

No. of ions on the basis of 2 oxygens

Si	0.000
Al	0.001
Ti	0.993
Fe	0.007
Mn	0.000
Mg	0.001
Zn	0.000
Cu	0.000
Sn	0.000
W	0.001
Ca	0.001
Na	0.002
K	0.000
Cl	0.000
F	0.000

Scheelite

	D7-22	D7-31
SiO_2	0.00	0.00
TiO_2	0.02	0.00
Al_2O_3	0.00	0.00
FeO	0.00	0.00
MnO	0.04	0.11
MgO	0.04	0.02
ZnO	0.00	0.00
CuO	0.04	0.04
SnO_2	0.04	0.04
WO_3	76.03	75.82
CaO	20.69	20.77
Na_2O	0.00	0.00
K_2O	0.02	0.00
Cl	0.02	0.04
F	1.38	1.39
MoO_3	0.45	1.01
Total	98.57	99.24

No. of ions on the basis of 4 oxygens

Si	0.000	0.000
Al	0.000	0.000
Ti	0.001	0.000
Fe	0.000	0.000
Mn	0.002	0.004
Mg	0.003	0.001
Zn	0.000	0.000
Cu	0.001	0.001
Sn	0.001	0.001
W	0.936	0.806
Ca	1.039	1.057
Na	0.000	0.000
K	0.001	0.000
Cl	0.001	0.003
F	0.206	0.209
Mo	0.027	0.020

Ilmenite

Sample No.:	D8-18	D7-62	D7-38
SiO_2	0.12	0.93	0.00
TiO_2	51.85	48.84	51.78
Al_2O_3	0.00	0.49	0.00
FeO	48.25	43.99	48.45
MnO	0.34	4.45	0.08
MgO	0.00	0.17	0.00
Cr_2O_3	0.00	0.00	0.00
NiO_2	0.00	0.00	0.00
CaO	0.01	0.12	0.00
SnO_2	0.02	0.08	0.04
Na_2O	0.00	0.00	0.00
K_2O	0.00	0.00	0.00
Total	100.60	99.08	100.35

No. of ions on the basis of 6 oxygen

Si	0.006		0.047		0.000	
Ti	1.955	1.96	1.854	1.93	1.940	1.94
Al	0.000		0.029		0.000	
Cr	0.000		0.000		0.000	
Fe^{+2}	1.945		1.690		1.973	
Mn	0.015	1.96	0.190	1.89	0.003	1.98
MgO	0.000		0.013		0.000	

Magnetite

	D7-18	D7-62	D7-39
SiO_2	0.48	0.34	2.03
TiO_2	0.22	0.72	0.37
Al_2O_3	0.13	0.19	0.10
FeO	31.46	31.36	30.55
Fe_2O_3	70.04	69.82	68.02
MnO	0.05	0.04	0.17
Cr_2O_3	0.00	0.00	0.00
NiO	0.00	0.00	0.00
CaO	0.04	0.07	0.24
SnO_2	0.08	0.00	0.05
Na_2O	0.00	0.00	0.00
K_2O	0.00	0.00	0.00
	102.50	102.54	101.53

No. of ions on the basis of 32 oxygens

Si	0.144		0.101		0.604	
Ti	0.049		0.161		0.083	
Sn	0.004	16.00	0.000	16.01	0.006	15.96
Al	0.045		0.067		0.035	
Fe^{3+}	15.762		15.677		15.227	
Fe^{2+}	7.869		7.828		7.600	
Mn	0.013	7.89	0.011	7.86	0.043	7.72
Ca	0.013		0.021		0.077	

Table 4

The compositions of primary minerals in Stage IB skarn and non-ore contact skarns. Pyroxene is from drill hole ML38 (D7-54 and D7-22) and ML40 (D7-80). Vesuvianites from ore skarn in ML38 (D7-55) ML47 (D7-71), ML41 (8-16 and D8-32). D7-80 comes from outside the ore skarn. Garnet comes from the skarn in ML38 (D7-56), ML41 (D8-35 and D8-16) and ML 2/5 (D8-4).

Pyroxene

Sample No.:	D7-80	D7-54	D7-22
SiO_2	50.08	51.01	52.33
TiO_2	0.01	0.05	0.21
Al_2O_3	1.37	0.63	1.45
FeO	13.82	15.12	7.34
MnO	0.66	0.53	0.35
MgO	9.67	8.36	13.08
ZnO	0.06	0.00	0.06
CuO	0.01	0.01	0.00
SnO_2	0.02	0.01	0.05
WO_3	0.06	0.00	0.15
CaO	22.46	23.88	24.76
Na_2O	0.02	0.16	0.05
K_2O	0.04	0.00	0.01
Cl	0.01	0.00	0.01
F	0.44	0.13	0.07
Total	98.74	99.87	99.92

No. of ions on the basis of 6 oxygens

Si	1.951	2.000	1.966	1.995	1.959	2.000
Al	0.049		0.029		0.041	
Al	0.014		0.000		0.023	
Ti^{+2}	0.001		0.001		0.006	
Fe^{+2}	0.450		0.487		0.230	
Mg	0.562		0.480		0.730	
Mn	0.022		0.002		0.011	
Zn	0.002		0.000		0.002	
Cu	0.000	2.047	0.000	1.978	0.000	2.011
Sn	0.000		0.000		0.001	
W	0.001		0.000		0.002	
Ca	0.937		0.986		0.993	
Na	0.001		0.006		0.004	
K	0.002		0.000		0.000	
Cl	0.001		0.000		0.001	
F	0.054		0.016		0.008	

Vesuvianite

	D8-32	D7-71	D8-16	D7-80	D7-55 core	D7-55 edge
SiO_2	36.92	34.85	36.08	37.80	35.56	35.37
TiO_2	3.26	1.60	0.84	0.96	4.27	3.51
Al_2O_3	12.95	13.83	14.37	17.01	11.91	12.26
FeO	4.86	6.71	6.79	6.71	6.17	5.32
MnO	0.18	0.47	0.51	0.34	0.21	0.21
MgO	2.83	1.82	2.07	0.11	1.98	2.87
ZnO	0.03	0.05	0.09	0.04	0.05	0.07
CuO	0.06	0.00	0.00	0.01	0.01	0.00
SnO_2	0.05	0.03	0.04	0.00	0.01	0.00
WO_3	0.00	0.15	0.00	0.08	0.10	0.00
CaO	35.31	34.16	35.2	34.93	34.77	34.89
Na_2O	0.05	0.05	0.06	0.05	0.11	0.06
K_2O	0.00	0.01	0.00	0.00	0.00	0.01
Cl	0.31	0.53	0.4	0.02	0.34	0.15
F	1.03	1.50	1.83	0.79	0.43	0.33
	100.00	100.00	100.00	100.00	100.00	100.00
Inferred OH	2.77	4.57	1.73	1.14	4.07	4.95

No. of ions on the basis of 76 (O, OH, F, Cl)

Si	17.564	18.000	16.439	18.000	17.663	18.000
Al	0.436		1.561		0.337	
Al	6.827		6.130		7.956	
Ti^{2+}	1.166		0.568		0.309	
Fe	1.933		2.648		2.780	
Mg	2.007		1.279		1.509	
Mn	0.072		0.187		0.212	12.447
Zn	0.011	12.049	0.017	10.837	0.032	
Cu	0.023		0.000		0.000	
Sn	0.010		0.003		0.009	
W	0.000		0.006		0.000	
Ca	17.999	18.045	17.266	17.317	18.465	18.524
Na	0.046		0.045		0.059	
K	0.000		0.006		0.000	
Cl	0.249	6.455	0.422	10.278	0.332	6.160
F	1.549		2.237		2.833	
OH	4.657		7.617		2.995	

Si	18.413	18.413	16.974	18.000	16.567	18.000
Al	0.000		1.026		1.433	
Al	9.769		5.676		5.470	
Ti^{2+}	0.351		1.533		1.237	
Fe	2.734		2.214		2.083	
Mg	0.079		1.408		2.004	
Mn	0.141	13.095	0.086	10.951	0.084	10.903
Zn	0.015		0.017		0.025	
Cu	0.003		0.003		0.000	
Sn	0.000		0.002		0.000	
W	0.003		0.012		0.000	
Ca	18.233	18.280	17.783	17.886	17.510	17.569
Na	0.047		0.103		0.056	
K	0.000		0.000		0.003	
Cl	0.018	3.200	0.275	7.790	0.118	8.804
F	1.218		0.648		0.490	
OH	1.964		6.867		8.196	

Garnet

	D8-35 edge	D8-16	D7-56 rim	D7-56 core	D8-4
SiO_2	37.44	37.50	34.51	35.69	35.74
TiO_2	0.38	0.44	5.42	3.89	0.61
Al_2O_3	12.41	11.50	5.44	8.98	5.16
Fe_2O_3	15.76	16.79	18.91	14.39	23.21
MnO	1.96	1.63	0.34	0.37	0.58
MgO	0.07	0.04	0.45	0.43	0.11
ZnO	0.04	0.04	0.01	0.00	0.02
CuO	0.01	0.03	0.04	0.00	0.00
SnO_2	0.12	0.16	0.51	0.15	0.38
WO_3	0.12	0.04	0.07	0.24	0.18
CaO	31.67	32.55	36.12	34.24	32.98
Na_2O	0.00	0.07	0.50	0.04	0.04
K_2O	0.00	0.00	0.01	0.01	0.01
Cl	0.01	0.01	0.05	0.01	0.00
F	0.16	1.10	0.05	0.00	0.36
	100.16	101.89	99.95	98.45	99.39

No. of ions on the basis of 24 oxygens

Si	5.940	6.000	5.874	6.000	5.652	6.000
Al	0.060		.126		0.348	
Al	2.261		1.998		0.702	
Ti^{3+}	0.045	4.188	1.979	4.029	2.330	3.700
Fe	1.882		0.052		0.668	
Mg	0.016		0.009		0.110	
Mn	0.263		0.216		0.047	
Zn	0.001	4.679	0.005	5.710	0.001	6.189
Cu	0.001		0.004		0.003	
Sn	0.009		0.011		0.037	
W	0.006		0.002		0.004	
Ca	5.384		5.463		5.987	
Na	0.000		0.100		0.159	
K	0.000		0.000		0.004	
Cl	0.003	0.083	0.003	0.548	0.014	0.040
F	0.080		0.545		0.026	

Si	5.189	6.000	5.934	6.000		
Al	0.181		0.066			
Al	1.546		0.943			
Ti^{3+}	1.766	3.789	2.900	3.919		
Fe	0.477		0.076			
Mg	0.105		0.027			
Mn	0.051		0.082			
Zn	0.000	6.182	0.002	6.057		
Cu	0.000		0.000			
Sn	0.011		0.028			
W	0.012		0.028			
Ca	5.983		0.009			
Na	0.018		5.867			
K	0.002		.0120			
			.0020			
Cl	0.002	0.003	0.000	0.189		
F	0.000		.1890			

060

735061

Table 5

The compositions of Stage II and Stage IB minerals. Amphibole compositions are from drill holes ML 2/1 (D7-65, D7-62 and D7-67), ML 2/5 (D8-10 and D8-7) and ML37 (D7-93). Sphene compositions are from ML 2/1 (D7-61), ML 2/5 (D8-9) and ML37 (D7-93). Analyses D7-22 come from Stage IB skarn in ML38. The Ilvaite analyses are from drill holes ML 2/1 (D7-64 and D7-65), and ML 2/5 (D8-7, D8-13 and D8-8).

Amphibole

Sample No.	D7-65	D7-62	D8-10	D8-7	D8-38	D7-93	D7-67	D8-10
SiO_2	39.07	37.61	39.89	37.68	38.56	37.65	54.60	39.89
TiO_2	0.29	0.60	0.23	0.58	0.60	0.23	0.05	0.20
Al_2O_3	9.55	11.32	10.67	14.79	10.22	12.11	0.43	10.67
FeO	28.14	29.25	24.92	26.40	31.25	26.41	13.99	24.92
MnO	0.48	0.46	0.49	0.45	0.51	0.55	0.76	0.49
MgO	3.50	1.93	5.01	2.65	1.25	3.98	14.86	5.01
ZnO	0.02	0.00	0.05	0.00	0.00	0.02	0.06	0.05
CuO	0.07	0.02	0.00	0.04	0.03	0.01	0.00	0.00
SnO_2	0.33	0.26	0.15	0.47	0.07	0.79	0.01	0.15
WO_3	0.00	0.01	0.00	0.00	0.00	0.00	0.06	0.00
CaO	11.03	10.81	11.56	11.33	11.02	11.15	11.85	11.50
Na_2O	1.65	1.66	1.70	1.50	1.31	1.85	0.14	1.70
K	1.38	1.46	1.37	1.50	1.79	1.71	0.10	1.37
Cl	0.78	0.84	0.44	0.55	1.05	1.71	0.02	0.44
F	0.63	0.64	0.21	0.18	0.18	0.51	0.90	0.11
Total	96.88	96.78	96.62	97.94	97.48	98.20	97.86	96.62
Inferred OH	3.12	2.22	3.38	2.06	2.52	1.80	2.14	3.38

On the basis of 24 oxygens

Si	6.586	8.000	6.068	8.000	6.162	8.000	5.912	8.000	6.165	8.000	5.956	8.000	7.873	7.496	5.888	7.744
Al	1.414		1.932		1.838		2.088		1.835		2.044		0.073		1.856	
Al	0.483	5.450	0.237	4.800	0.106	4.578	0.655	4.694	0.100	4.790	0.218	4.782	0.000	4.983	0.000	5.351
Ti	0.036		0.079		0.028		0.068		0.072		0.028		0.006		0.026	
Fe^{+2}	3.963		3.956		3.219		3.473		4.178		3.496		1.688		4.152	
Mn	0.068		0.063		0.060		0.060		0.069		0.074		0.093		0.061	
Mg	0.879		0.466		1.154		0.621		0.298		0.936		3.193		1.102	
Zn	0.000		0.000		0.006		0.000		0.000		0.000		0.000		0.000	
Cu	0.005		0.000		0.000		0.000		0.000		0.000		0.000		0.000	
Sn	0.012		0.009		0.005		0.017		0.002		0.028		0.001		0.010	
W	0.000		0.000		0.000		0.000		0.000		0.000		0.002		0.000	
Ca	1.993	2.828	1.874	2.698	1.904	2.692	1.909	2.868	1.888	2.658	1.885	2.803	1.831	1.890	1.818	2.309
Na	0.539		0.521		0.519		0.458		0.405		0.567		0.040		0.243	
K	0.296		0.301		0.269		0.301		0.365		0.346		0.019		0.247	
Cl	0.222	2.099	0.329	1.756	0.115	1.961	0.278	1.450	0.284	1.798	0.458	1.729	0.005	1.506	0.110	1.971
F	0.336		0.328		0.103		0.090		0.091		0.265		0.411		0.098	
OH	1.541		1.199		1.741		1.081		1.423		1.006		1.090		1.763	

Sphene

	D7-60	D7-61 edge	D7-61 centre	D8-9	D7-22 edge	D7-22 centre	D7-93
SiO_2	29.91	30.59	30.34	30.27	30.76	30.77	30.47
TiO_2	27.40	32.04	32.44	26.98	31.5*	33.40	28.52
Al_2O_3	1.21	2.86	2.84	7.49	4.46	1.45	6.46
Fe_2O_3	2.17	1.54	1.44	1.40	0.59	0.58	1.01
FeO	0.02	0.04	0.06	0.06	0.03	0.00	0.01
MnO	0.00	0.08	0.04	0.04	0.04	0.02	0.02
MgO	0.05	0.06	0.00	0.00	0.00	0.05	0.06
ZnO	0.04	0.00	0.00	0.00	0.02	0.01	0.07
CaO	9.26	2.21	2.07	0.63	0.94	1.69	0.28
SnO_2	0.00	0.00	0.10	0.11	0.09	0.06	0.13
WO_3	26.07	27.56	27.54	28.50	28.11	28.80	28.27
CuO	0.07	0.02	0.07	0.05	0.03	0.00	0.00
Na_2O	0.01	0.50	0.01	0.01	0.00	0.01	0.01
K_2O	0.00	0.00	0.00	0.00	0.01	0.01	0.00
Cl	0.14	1.93	1.44	2.91	2.82	0.47	1.05
F							
Total	95.65	98.91	98.29	98.46	99.47	99.50	98.40
Inferred OH	3.35	1.07	1.71	1.54	0.53	0.50	1.60

On the basis of 20 oxygens

Si	4.008	4.008	3.991	3.991	3.922	3.922	3.857	3.857	3.983	3.982	4.024	4.024	3.875	3.875		
Al	0.000		0.009		0.078		0.143		0.017		0.000		0.125			
Al	0.191	1.759	0.440	3.908	0.424	3.869	1.125	3.913	0.681	3.889	0.532	3.992	0.921	3.846		
Ti	2.760		3.144		3.154		2.585		3.074		3.285		2.728			
Fe	0.243		0.169		0.155		0.149		0.067		0.064		0.108			
Mn	0.002		0.005		0.006		0.006		0.003		-		0.001			
Mg	0.000		0.016		0.007		0.009		0.007		0.004		0.004			
Zn	0.005		0.006		0.000		0.000		0.000		0.004		0.005			
Cu	0.004		0.000		0.000		0.000		0.002		0.003		0.007			
Sn	0.553		0.129		0.120		0.036		0.055		0.098		0.016			
W	0.000		0.000		0.003		0.004		0.003		0.002		0.004			
Ca	1.743	3.762	1.853	3.858	1.815	3.834	1.891	3.905	1.898	3.906	1.935	4.036	1.852	3.854		
Na	0.018		0.005		0.017		0.012		0.008		0.000		0.002			
K	0.001		0.000		0.002		0.002		0.000		0.001		0.000			
Cl	0.000	1.647	0.000	1.290	0.000	1.371	0.000	1.867	0.003	1.401	0.002	0.810	0.000	1.945		
F	0.060		0.797		0.589		1.173		1.155		0.277		1.226			
OH	1.587		0.493		0.782		0.694		0.241		0.231		0.719			

Ilvaite

	D8-7	D7-64	D7-65	D8-13	D8-8
SiO_2	28.5	29.38	28.61	29.01	29.41
TiO_2	3.79	5.99	4.98	4.52	4.43
Al_2O_3	7.3	2.70	4.37	5.22	4.67
Fe_2O_3	15.43	15.13	15.04	15.10	15.03
FeO	27.72	27.12	27.02	27.22	26.93
MnO	0.39	0.39	0.38	0.45	0.43
MgO	0.7	0.41	0.46	0.81	0.84
ZnO	0.08	0.08	0.07	0.08	0.00
CuO	0.05	0.05	0.00	0.02	0.01
SnO_2	0.41	1.08	0.49	0.6	0.70
WO_3	0.00	0.00	0.00	0.04	0.12
CaO	12.69	12.77	13.01	13.1	12.85
Na_2O	0.22	0.32	0.19	0.13	0.28
K_2O	0.01	0.00	0.00	0.00	0.00
Cl	0.01	0.00	0.00	0.00	0.00
F	0.00	0.28	0.27	0.00	0.37
Total	96.92	95.90	94.63	95.85	95.04
Inferred OH	3.08	4.10	5.37	4.15	4.36

On the basis of 9 oxygens

Si	1.799	2.000	1.8524	2.000	1.754	2.000	1.805	2.000	1.867	2.000						
Al	0.201		0.1476		0.246		0.195		0.133							
Al	0.342	1.255	0.057	1.055	0.070	0.99-	0.188	1.460	0.216	1.46						
Ti	0.180		0.284		0.226		0.211		0.212							
Fe^{3+}	0.733		0.718		0.694		1.061		0.716							
Fe^{2+}	1.463	1.567	1.430	1.526	1.386	1.470	1.416	1.538	1.430	1.554						
Mn	0.021		0.021		0.020		0.024		0.023							
Mg	0.066		0.039		0.042		0.075		0.079							
Zn	0.004		0.004		0.003		0.004		0.000							
Cu	0.002		0.002		0.000		0.001		0.000							
Sn	0.011		0.030		0.015		0.017		0.020							
W	0.000		0.000		0.000		0.001		0.002							
Ca	0.858	0.886	0.863	0.902	0.855	0.878	0.873	0.889	0.876	0.908						
Na	0.027		0.039		0.023		0.016		0.034							
K	0.001		0.000		0.000		0.000		0.000							
Cl	0.001	0.688	0.000	0.970	0.000	1.216	0.000	0.912	0.000	0.828						
F	0.000		0.056		0.052		0.000		0.074							
OH	0.687		0.914		1.164		0.912		0.754							

Plate I

Primary Stage IA skarn textures and some arrested Stage IA to Stage IIA textures.

A. Magnetite "atoll" texture with siderite (Sid). The atolls often contain siderite but may contain cassiterite or, rarely, K-feldspar (from drill hole 38, 100X).

B. Euhedral magnetite + quartz + cassiterite + K-feldspar in siderite matrix in unaltered stage IA skarn (from drill hole 38, 100X).

C. Cassiterite relicts within a Stage IIA amphibole host (Sn-ferro-hastingsite). The corroded relicts are all optically continuous. The suggested form of the pseudomorph is similar to the shape of cassiterite crystals in Stage IA skarn - see Plate IB. (From near the top of the skarn intersection in drill hole 41, at the stage IIA Boundary (100X).

D. Cassiterite relicts in a biotite (F-annite) host. The different relicts are again optically continuous. It comes from near where the sample shown in last photomicrograph comes from (400X).

E. Euhedral ilmenite (Im) in siderite matrix. Magnetite typically shows atoll texture. Note the lack of exsolution in the oxide minerals (from drill hole 38, 400X; in reflected light and oil immersion).

F. Relict ilmenite crystal mantled by Sn-sphene (sph) in amphibole (Stage IB) skarn. From drill hole 37 (100X).

Mag
Std
A
Kf
Mag
Cas
Qtz
Std
B
Cas
Amp
C
Cas
Bio
D
Mag
Ilm
E
Ilm
Sph
F

Plate II

Stage II skarn textures showing various relict stage I skarn features.

A. Essentially unaltered radiating vesuvianite (Ves.) within Stage II(?) magnetite overprint (from drill hole 41, 100X)

B. Vesuvianite largely altered to amphibole (Amph) within stage II(?) magnetite overprint (from the same polished thin section as A, 100X).

C. Stage IB, euhedral Ti-andradite garnets (Gar) within stage II(?) magnetite overprint. The upper crystal is nearly completely altered to amphibole while the other lower one is only partly altered (drill hole 47, 40X).

D. Stage IIB Sn-ilvaite (Ilv) occurring, mantling altered magnetite. Such magnetite may well be related to Stage IIA skarn genesis. Tabular crystals of ilvaite project into late fluorite (drill hole 2/5, 100X).

E. Colour zoned amphibole crystals within late anhedral quartz. The paler outer zone of the amphiboles is Mg-rich tremolite actinolite while the darker inner zones are Mg-poor ferrohastingsite. (Drill hole 47, 40X).

F. Radiating siderite spherulite in a massive siderite matrix. The darker outer edge of the spherulite is stilpnomelane. This texture was only observed near the stage IA-IIA skarns' contact (from the top of drill hole 41, 100X).

Ves
Mag
A
Ves
Amph
Mag
B
Mag
Gar
C
Qtz
Sph
Ilv
Amph
Mag
D
Qtz
Pale Amph
Green Amph
E
Sid
Mag
Stil
F

Plate III

Zoning in Stage II and Stage IA skarns

A. The original, pre-replacement units in B, below. The sample comes from the bottom contact of the No. 2 skarn unit; drill hole 2/5. The sample is of drill core, approximately 3.5 centimetres wide.

B. Photo of a partly replaced (Stage II) equivalent to A.

C. The replacement and vein features of A. Fractures have not been shown. The zoning is clearly related to fractures representing permeable areas during skarn genesis.

D. A photo of stage IA skarn. The sample is also approximately 3.5 centimetres wide, from drill hole 38.

E. The various veins and zones of "D" above. Although at least three periods of fracturing are evident zones A, B and C appear to relate mainly to the second set of veins. Zone A contains K-feldspar. The other two do not. Zone C is distinct from Zone B by the former containing much more siderite.

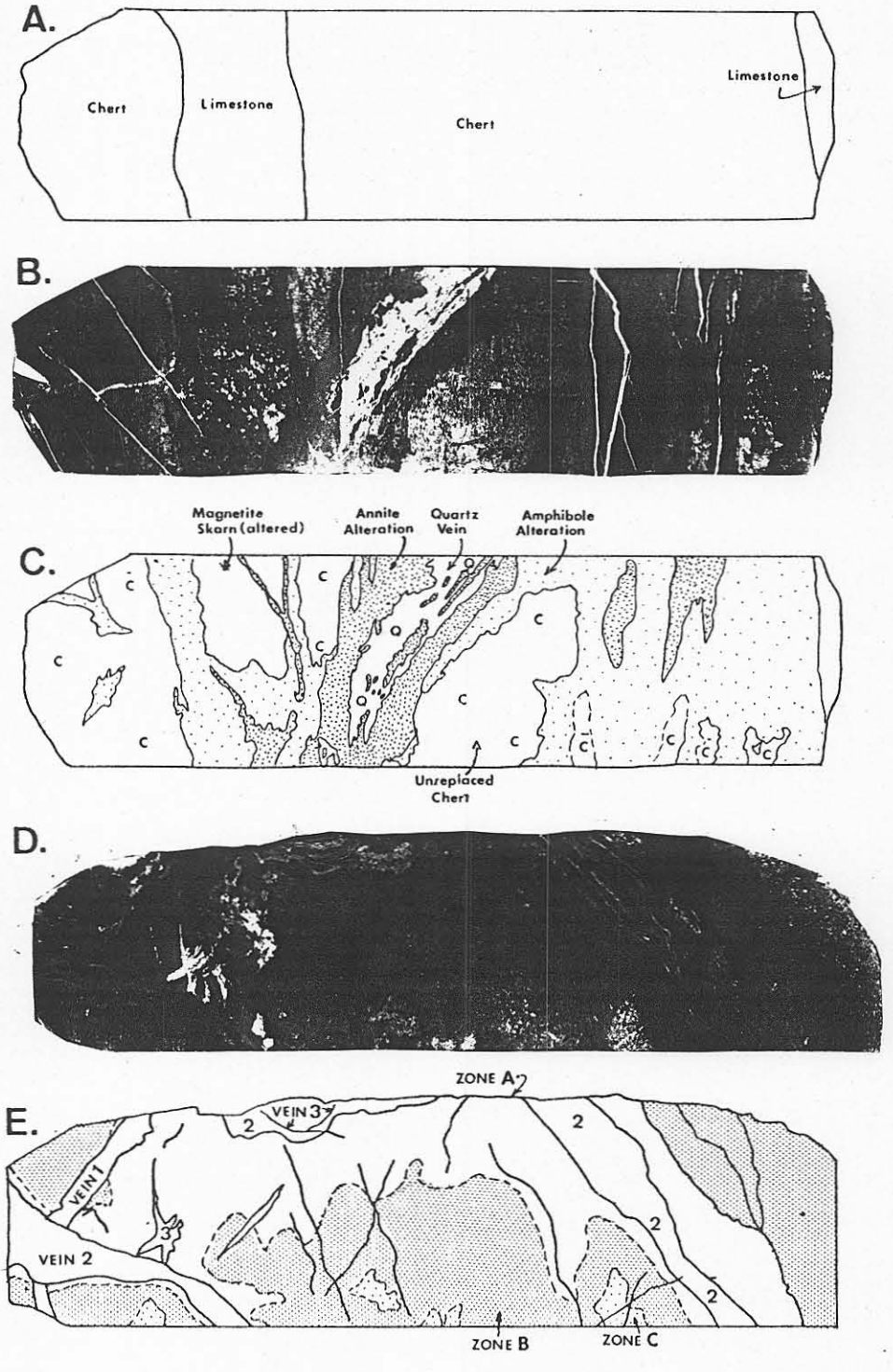
A.
Chert
Limestone
Chert
Limestone
B.
C.
Magnetite Skarn (altered)
Annite Alteration
Quartz Vein
Amphibole Alteration
Unreplaced Chert
D.
E.
ZONE A
VEIN 3
VEIN 1
VEIN 2
ZONE B
ZONE C

ACKNOWLEDGEMENTS

The author wishes to thank Mr. L. Newnham, the Renison-Goldfields Co. Ltd. and Aberfoyle Co. Ltd. for access to company data and drill core without which a study of this type would be impossible.

Mr. David Sewell and Mr. Pat Kelly of the University of Melbourne are thanked for help with the electron microprobe analyses. Mrs. Judith Egan and Mrs. Jane Morris are thanked for drafting and typing help, respectively.

REFERENCES

Atkinson, W.W., Jr., and Einaudi, M.T., 1978, Skarn formation and mineralization in the contact aureole at Carr Fork, Bingham, Utah: ECON. GEOL., v. 73, p. 1326-1365.

Barraclough, P., 1979, Geological investigations at the Molyhill Scheelite Mine, Central Australia: N.T. Geol. Survey, G.S. 79. Ituchita 1:250,000 sheet area. SF/53-11, p. 14.

Bateman, P.C., 1965, Geology and tungsten mineralization of the Bishop district, California: U.S. Geol. Survey Prof. Paper 470, 208 p.

Buseck, P.R., 1967, Contact metasomatism and ore deposition: Tem Piute, Nevada: ECON. GEOL., v. 62, p. 331-353.

Collins, P.L.F., 1981, The geology and genesis of the Cleveland tin deposit, Western Tasmania: Fluid inclusion and stable isotope studies: ECON. GEOL., v. 76, p. 365-392.

Collins, W.J., Beams, S.D., White, A.J.R. and Chappell, B.W., 1982, Nature and origin of A-type granites with particular reference to southeastern Australia: Contr. Mineral. Petrol. (*in press*).

Deer, W.A., Howie, R.A. and Zussman, J., 1962, Rock Forming Minerals: Longmans, Green and Co. Ltd., London, v. 1-5.

Eadington, P.J. and Giblin, A., 1979, Alteration minerals and the precipitation of tin in granitic rocks: C.S.I.R.O. Division of Mineralogy, Technical Communication 68, 31 p.

French, B.M., 1971, Stability relations of siderite ($FeCO_3$) in system Fe-C-O: Am. Jour. Sci., v. 271, p. 37-78.

Groves, D.I., Martin E.L., Murchies, H., and Wellington, H.K., 1972, A century of tin mining at Mt. Bischoff, 1871-1971: Bull. geol. Survey, Dept. Mines, Tasmania, No. 54, 197 p.

Jessop, A., 1969, Report on the summer exploration program undertaken at Mt. Lindsay, Tasmania, 1968-1969; Aberfoyle Tin Development Partnership Report.

John, Y.W., 1978, Geology and origin of Sangdong tungsten mine, Republic of Korea: ECON. GEOL., v. 58, p. 1285-1300.

Kelly, W.C. and Turneaure, F.S., 1970, Mineralogy, paragenesis and geothermometry of the tin and tungsten deposits of the Eastern Andes, Bolivia: ECON. GEOL., v. 5, p. 609-680.

Kinealy, K., 1979, Chemical analyses of samples from the Mt. Lindsay deposit, Tasmania. C.S.I.R.O. Restricted Investigation Report 1002, 8 p.

Korzhinskii, D.S., 1964, An outline of metasomatic processes: Internat. Geol. Rev., v.6, p. 1713-1734, 1920-1952, 2169-2198.

Korzhinskii, D.S., 1970, Theory of metasomatic zoning: Oxford Clarendon Press, 162 p.

Kwak, T.A.P., 1982, Sector-zoned $annite_{85}$ $phlogopite_{15}$ micas from the Mt. Lindsay Sn-W-F(-Be) deposit, Tasmania, Australia: Can. Min., v. 19, p. 643-650.

Kwak, T.A.P. and Askins, P.W., 1981a, Geology and genesis of the F-Sn-W(-Be) skarn (wrigglite) at Moina, Tasmania: ECON. GEOL. v. 79, p. 439-467.

Kwak, T.A.P. and Askins, P.W., 1981b, The nomenclature of carbonate replacement deposits, with emphasis on Sn-F(-Be-Zn) "wrigglite" skarns: Jour. geol. Soc. Aust., v. 28, p. 123-136.

Kwak, T.A.P. and Tan, T.H., 1981, The geochemistry of zoning in skarn minerals at the King Island (Dolphin) mine: ECON. GEOL., v. 76, p. 468-497.

Kwak, T.A.P., Taylor, R.G. and Plimer, I.R., 1982, The occurrence and genesis of primary tungsten deposits in Australia: Monogram, Mineralization Aossicated with Acid Magmatism group (W.A.M.A.W.) (*in press*).

Lindsley, D.H., 1963, Magnetite-ilmenite relations below 1000°C: Carnegie Inst. Wash. Yearb., 6R, p. 60-66.

Morrison, G.W., 1981, Setting and origin of skarn deposits in the Whitehorse Copper Belt, Yukon: Unpub. PhD thesis, Univ. Western Ontario, Ont., Canada, 308 p.

Nockleberg, W.J., 1981, Geologic setting, petrology and geochemistry of zoned tungsten-bearing skarns at the Strawberry Mine, Central Sierra Nevada, California: ECON. GEOL., v. 76, p. 111 - 133.

Patterson, D.J., Ohmoto, H., and Solomon, M., 1981, Geologic setting and genesis of cassiterite-sulfide mineralization at Renison Bell, Western Tasmania: ECON. GEOL., v. 76, p. 393-438.

Sato, K., 1980, Tungsten skarn deposit of the Fujigatani mine, Southwestern Japan: ECON. GEOL., v. 75, p. 1066-1082.

Takenouchi, S., 1971, Hydrothermal synthesis and consideration of the genesis of Malayaite: Mineral Deposita., v. 6, p. 335-347.

Taylor, B.E., 1976, Origin and significance of C-O-H fluids in the formation of Cu-Fe-Si skarn, Osgood Mountains, Humbolt Country, Nevada: Unpub.. PhD thesis, Stanford Univ., 230 p.

Taylor, B.E. and O'Neill, J.R., 1977, Stable isotope studies of metasomatic Ca-Fe-Al-Si skarns and associated metamorphic and igneous rocks, Osgood Mtns, Nevada: Contr. Mineral. Petrol., v. 63, p. 1-49.

Umpleby, J.B., 1916, The occurrence of ore on the limestone side of garnet zones: Calif. Univ. Dept. Geol. Bull., v. 10, p. 25-37.

Wolff, A., 1978, The Kara deposit, in "Geology and mineralization of N.W. Tasmania": Geol. Soc. Aust. Symposium on the geology and mineralization of N.W. Tasmania, Burnie, p. 37-38.

Wones, D.R. and Eugster, H.P., 1965, Stability of biotite : experiment theory, and application: Am. Min., v. 50, p. 1228-1272.

Zharikov, V.A., 1970, Skarns: Internat. Geol. Rev., v. 12, p. 541-559, 619-647, 760-775.